Tree Physiology 00, 1–19
https://doi.org/10.1093/treephys/tpab021

Research paper

Different climate sensitivity for radial growth, but uniform for tree-ring stable isotopes along an aridity gradient in *Polylepis tarapacana*, the world's highest elevation tree species

Milagros Rodriguez-Caton[1,11], Laia Andreu-Hayles[1,2,3], Mariano S. Morales[4,5], Valérie Daux[6], Duncan A. Christie[7,8], Rafael E. Coopman[9], Claudio Alvarez[7], Mukund Palat Rao[1,10], Diego Aliste[7,8], Felipe Flores[7] and Ricardo Villalba[4]

[1]Lamont-Doherty Earth Observatory, Columbia University, 61 Route 9W, Palisades, NY 10964, USA; [2]CREAF, Bellaterra (Cerdanyola del Vallés), Barcelona, Spain; [3]ICREA, Pg. Lluís Companys 23, Barcelona, Spain; [4]Instituto Argentino de Nivología, Glaciología y Ciencias Ambientales (IANIGLA), CONICET, Av. Ruiz Leal s/n, Mendoza 5500, Argentina; [5]Laboratorio de Dendrocronología, Universidad Continental, Av. San Carlos 1980, Huancayo 12003, Perú; [6]Laboratoire des Sciences du Climat et de l'Environnement, CEA/CNRS/UVSQ/IPSL, Gif-sur-Yvette, France; [7]Laboratorio de Dendrocronología y Cambio Global, Instituto de Conservación Biodiversidad y Territorio, Universidad Austral de Chile, Campus Isla Teja, Valdivia 5110566, Los Ríos, Chile; [8]Center for Climate and Resilience Research, (CR)2, Blanco Encalada 2002, Santiago 8370415, Chile; [9]Ecophysiology Laboratory for Forest Conservation, Instituto de Conservación, Biodiversidad y Territorio, Facultad de Ciencias Forestales y Recursos Naturales, Universidad Austral de Chile, Independencia 631, Valdivia 5110566, Los Ríos, Chile; [10]Department of Earth and Environmental Sciences, Columbia University, 5th Floor Schermerhorn Extension, 1200 Amsterdam Ave., New York, NY 10027, USA; [11]Corresponding author (milagros@ldeo.columbia.edu; milagrosrodriguezc@gmail.com);

Received December 7, 2020; accepted February 2, 2021; handling Editor Lucas Cernusak

Tree growth is generally considered to be temperature limited at upper elevation treelines, yet climate factors controlling tree growth at semiarid treelines are poorly understood. We explored the influence of climate on stem growth and stable isotopes for *Polylepis tarapacana* Philipi, the world's highest elevation tree species, which is found only in the South American Altiplano. We developed tree-ring width index (RWI), oxygen ($\delta^{18}O$) and carbon ($\delta^{13}C$) chronologies for the last 60 years at four *P. tarapacana* stands located above 4400 m in elevation, along a 500 km latitude aridity gradient. Total annual precipitation decreased from 300 to 200 mm from the northern to the southern sites. We used RWI as a proxy of wood formation (carbon sink) and isotopic tree-ring signatures as proxies of leaf-level gas exchange processes (carbon source). We found distinct climatic conditions regulating carbon sink processes along the gradient. Current growing-season temperature regulated RWI at northern-wetter sites, while prior growing-season precipitation determined RWI at arid southern sites. This suggests that the relative importance of temperature to precipitation in regulating tree growth is driven by site water availability. By contrast, warm and dry growing seasons resulted in enriched tree-ring $\delta^{13}C$ and $\delta^{18}O$ at all study sites, suggesting that similar climate conditions control carbon-source processes along the gradient. Site-level $\delta^{13}C$ and $\delta^{18}O$ chronologies were significantly and positively related at all sites, with the strongest relationships among the southern drier stands. This indicates an overall regulation of intercellular carbon dioxide via stomatal conductance for the entire *P. tarapacana* network, with greater stomatal control when aridity increases. This manuscript also highlights a coupling (decoupling) between physiological processes at leaf level and wood formation as a function of similarities (differences) in their climatic sensitivity. This study contributes to a better understanding and prediction of the response of high-elevation *Polylepis* woodlands to rapid climate changes and projected drying in the Altiplano.

Keywords: carbon reserves, Central Andes, drought stress, dryness, evaporative enrichment, lagged response.

Introduction

The highest treelines in the world are located in mid to low latitudes in the rather dry mountains of the South American Altiplano and eastern Tibet. The existence of trees at these extreme locations has been associated with higher solar radiation and warmer mean temperature (T) compared with high-elevation humid tropics (Körner 1998). At upper elevation treelines, tree radial growth is generally limited by growing season T, which restricts meristematic activity (Shi et al. 2008). However, tree growth can be regulated by water availability at drier treelines (Morales et al. 2004, Piper and Fajardo 2011, Liang et al. 2014). In addition, the tree-growth response to summer T has weakened or even disappeared in the last few decades at some high-latitude Northern Hemisphere forests (D'Arrigo et al. 2008), suggesting that moisture stress induced by increasing temperature could have gained relevance.

In the last decades, persistent warming and drying trends have been observed at high-elevation mountains in the Central Andes (Vuille and Bradley 2000, Vuille et al. 2015) and are expected to continue into the future (Minvielle and Garreaud 2011, Thibeault et al. 2012, Neukom et al. 2015). Under this scenario, a potential significant reduction of the spatial distribution of *Polylepis tarapacana* Philipi is expected to occur during the present century, especially for drier or lower-elevation stands (Cuyckens et al. 2016). Therefore, a better ecological and physiological understanding of *P. tarapacana* forests is urgently needed to more accurately predict its climate sensitivity and improve conservation policies for these high-elevation ecosystems.

The genus *Polylepis* comprises small- to medium-sized evergreen angiosperm trees that span large high-elevation areas in the Andes in South America from 8° N to 32° S (Gosling et al. 2009, Zutta and Rundel 2017, Cuyckens and Renison 2018). Among all *Polylepis* species, *P. tarapacana* (Figure 1a) occurs in the harshest conditions in the semiarid Central Andean Altiplano (Toivonen et al. 2014) and forms the highest-elevation treeline worldwide (~5100 m above sea level (a.s.l.), Braun 1997) with some individuals reaching up to 5255 m a.s.l. (Salar de Surire, Chile, personal observations). *P. tarapacana* is a small evergreen tree species of 0.5–4 m height. It is distributed in monospecific patches of open woodlands on the slopes of mountains and volcanoes across the Altiplano region from 17.5° S to 23.5° S in Peru, Bolivia, Chile and Argentina above 4000 m a.s.l. (Cuyckens et al. 2016).

P. tarapacana has species-specific traits that aid its survival in extremely dry, cold, windy and high solar radiation environments. It has advanced photoprotective mechanisms to reduce photodamage (García-Plazaola et al. 2015). Its leaves are thick and small, and are covered by waxes and a thick pubescent layer (Gonzalez et al. 2002, Macek et al. 2009). It is an isohydric species that rapidly closes its stomata when soil moisture decreases and air vapor pressure deficit (VPD) increases. *P. tarapacana*'s stomata are arranged in crypts with trichomes, a trait often considered a xerophytic adaptation to aridity. This feature increases water-use efficiency via enhanced boundary layer resistance and facilitates diffusion of carbon dioxide (CO_2) to mesophyll cells (Jordan et al. 2008, Hassiotou et al. 2009). Due to these adaptations, the photosynthetic activity of *P. tarapacana* can occur under higher VPD levels than other treeline species (Simpson 1979, Haworth and McElwain 2008). *P. tarapacana* also has frost tolerance and frost avoidance mechanisms. It can resist temperatures up to approximately −20 °C without tissue damage (Rada et al. 2001, Azocar et al. 2007). Its supercooling capacity avoids freezing and keeps an active metabolism at temperatures from −3 to −6 °C and from −7 to −9 °C during the dry-cold and wet-warm seasons, respectively (Rada et al. 2001). Similar to other *Polylepis* species, the bark of *P. tarapacana* has multiple layers that insulate the stem from freezing temperatures.

Both precipitation (PP) and T exert large influences on *P. tarapacana*, but assessing which is the dominant limiting factor governing growth and ecophysiological patterns remains challenging. *P. tarapacana* tree establishment occurs mainly at specific microsites near or under rocks (López et al. 2021). Rocks protect *Polylepis* seedlings against desiccant winds and low temperatures, provide shading that decreases evaporation and collect water down slope (Kleier and Rundel 2004). *Polylepis tarapacana*'s maximum tree height, annual shoot increment and mean tree-ring width have been shown to decrease with elevation, therefore with decreasing T (Hoch and Körner 2005, Kessler et al. 2007, Domic and Capriles 2009, Macek et al. 2009). However, at daily scales, higher T and midday maximum VPD limit carbon assimilation in this species by inducing stomatal closure (García-Plazaola et al. 2015).

Dendrochronological studies at different elevations have reported a high coherency of interannual growth variations among a wide spatial network of *P. tarapacana* ring-width chronologies over the past centuries (Argollo et al. 2004, Soliz et al. 2009). These studies have indicated previous growing-season PP as the main driver of interannual ring-width variability. This moisture signal in tree-ring width has been leveraged to reconstruct hydroclimatic variability for the last centuries in this region (Morales et al. 2012, 2015, 2020). The *P. tarapacana* ring-width network also showed a negative effect of previous-growing season T over radial growth (e.g., Soliz et al. 2009). As higher T reduces soil moisture by increasing evaporation, this is consistent with the negative influence of dry conditions on radial growth (Morales et al. 2004). This response of tree growth to moisture conditions agrees with *P. tarapacana*'s arid environment with ~100–450 mm of total annual PP along its distribution (Kessler 1995, Cuyckens et al. 2016).

Surprisingly, and contrary to the observed relationships with climate of the previous growing season, current growing-season

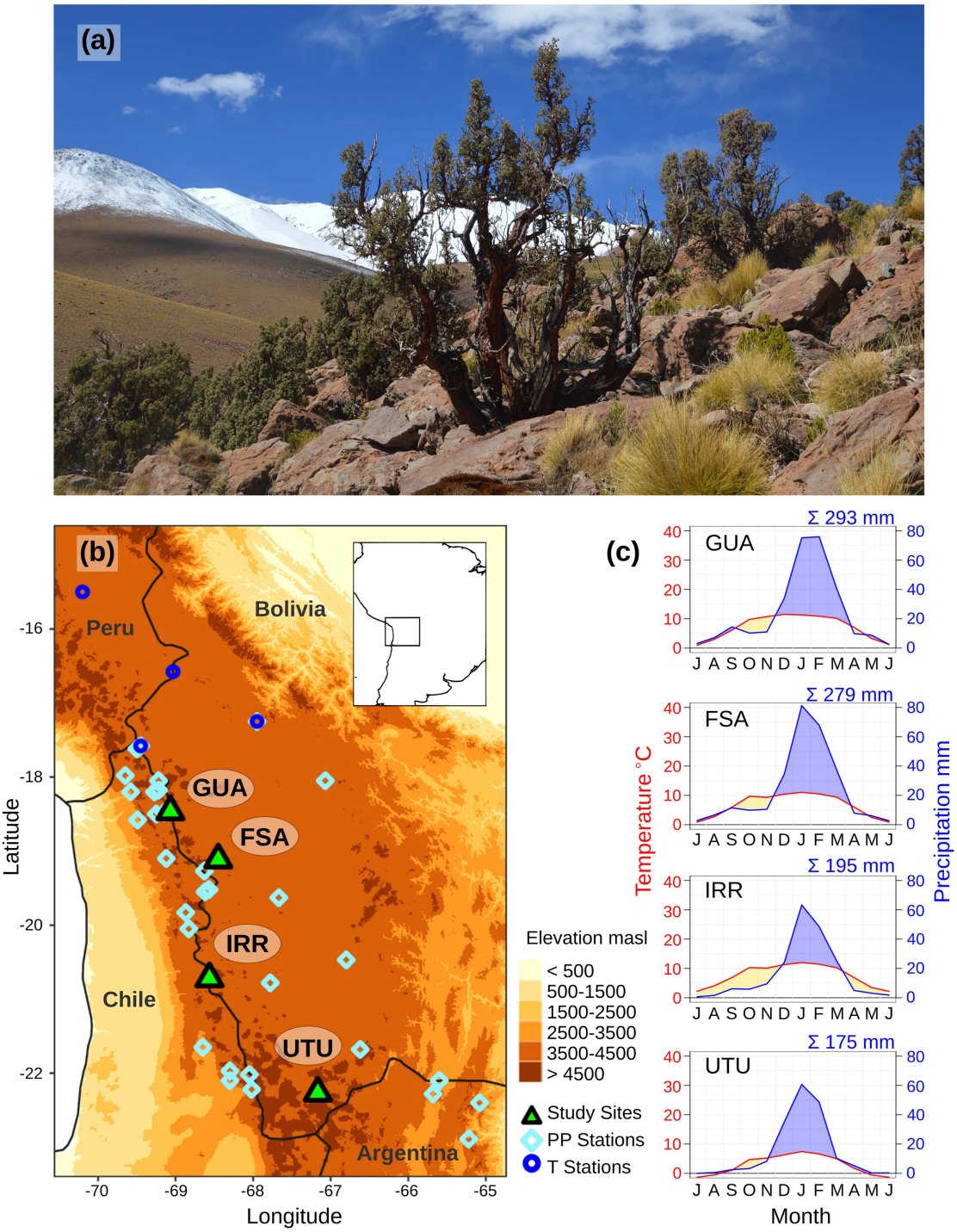

Figure 1. (a) *Polylepis tarapacana* in Uturunco, Bolivia (22°18′ S, 67°14′ W, 4600 m a.s.l.). (b) Location of the four *Polylepis tarapacana* study sites (green triangles): Guallatire (GUA), Frente Sabaya (FSA), Irruputuncu (IRR) and Uturunco (UTU), and meteorological stations for precipitation (PP) (light blue diamonds) and temperature (T) (dark blue circles). Background colors represent elevation in meters above sea level (m a.s.l.). (c) Annual cycle of T (red line) and PP (blue line) for each site based on the ERA interim product (1979–2018) and CHIRPS data set (1981–2018), respectively; mean total annual precipitation for each site is reported on the top right-hand corner of each panel.

T seems to favor radial growth and current growing-season PP seems to be growth detrimental (Argollo et al. 2004, Christie et al. 2009, Moya and Lara 2011). Part of this contrasting pattern may be explained by the strong negative correlation between PP and T during summer months, since the presence of clouds decreases T considerably at these high-elevation environments (Figure S1 available as Supplementary data at *Tree Physiology* Online). However, the underlying

physiological processes associated with the lagged response of growth as well as the apparent opposite growth-climate sensitivities between previous and current year remain unexplained. Exploring other tree-ring parameters such as stable isotope ratios across environmental gradients represents an alternate and promising approach to better understand *P. tarapacana* ecophysiology.

Oxygen ($\delta^{18}O$) and carbon ($\delta^{13}C$) stable isotopes in tree rings provide complementary information on ecophysiological responses to environmental changes and have been shown to be more sensitive to current growing-season climate than tree-ring width index (RWI) for a variety of species and sites (e.g., Andreu et al. 2008, Lavergne et al. 2018, Awada et al. 2019). Tree-ring $\delta^{18}O$ reflects source water $\delta^{18}O$ that is modulated by evaporative enrichment occurring at leaf level during transpiration. This enrichment depends on the vapor pressures of the intercellular air spaces of the leaf, the leaf surface (which depends notably on the stomatal conductance) and the bulk air (e.g., Roden et al. 2000, Barbour 2007, Gessler et al. 2014). The $\delta^{13}C$ ratios in tree-ring cellulose are inherited from the original values of $\delta^{13}C$ in the atmospheric CO_2 modified by fractionation occurring at the leaf level and, to a lesser extent, by postphotosynthetic processes. During CO_2 diffusion through stomata, ^{12}C-bearing molecules exhibit higher diffusivity than ^{13}C, resulting in a higher carboxylation rate of ^{12}C relative to ^{13}C. If the stomatal conductance is high compared with the velocity of Rubisco carboxylation, the internal concentration of CO_2 in the leaf is high, and there is strong discrimination against ^{13}C that leads to low $\delta^{13}C$ ratios. Conversely, when the stomatal conductance is low compared with the rate of CO_2 assimilation, the discrimination against ^{13}C is lower, leading to high $\delta^{13}C$ (e.g., Cernusak et al. 2013). Hence, fractionation processes are related to the ratio of internal to external concentrations of CO_2 in the leaf and thus reflect a balance between velocity of Rubisco carboxylation and stomatal conductance (e.g., Farquhar et al. 1982, Cernusak et al. 2013). Combining $\delta^{13}C$ and $\delta^{18}O$ provides insights into a plant's CO_2 assimilation rate in relation to its stomatal conductance (Scheidegger et al. 2000, Grams et al. 2007).

Here, we analyzed *P. tarapacana* responses to climate for the period 1950–2008 using RWI, $\delta^{18}O$ and $\delta^{13}C$ tree-ring chronologies developed at four sites along a 500 km latitudinal aridity gradient. The specific questions we address are as follows: (i) How and when do climate conditions influence interannual variation in *P. tarapacana* radial growth and stable isotopes ratios? (ii) Are climate controls on wood formation (carbon sink) and leaf-level gas exchange (carbon source) similar along the gradient? (iii) Which mechanisms can explain the relationships between growth and prior-year climate conditions? Addressing these questions will help us to understand the potential sensitivity of high-elevation *Polylepis* populations to climate change.

Materials and methods

Study sites and climate

Along the South American Altiplano (16° S—23° S), there is a significant decrease in PP from north to south (Vuille and Keimig 2004). In the northern and wetter regions of the species distribution, *P. tarapacana* forest patches cover wider areas than in the south. While in the north the patches are uniformly distributed around the volcanoes, in the south, they are mostly located in north, northeast and east facing slopes. The *P. tarapacana* patchy distribution seems to be more related to topographic and microclimatic conditions than to human activities, as has been described for other *Polylepis* species (Kessler 1995).

Four *P. tarapacana* open woodland locations were selected along the latitudinal aridity gradient spanning from 18° S to 22° S in the Altiplano in South America (Figure 1b, Table 1). Sampling sites were located above 4400 m a.s.l. on moderate slopes and rocky volcanic soils. At this elevation, air temperatures are frequently below 0 °C during the night, even in summer (Macek et al. 2009). Additionally, daily diurnal thermal amplitudes (~17 °C) are larger than seasonal amplitudes (~4–10 °C) (Patacamaya weather station, Garcia et al. 2007). The sampling strategy targeted woodland patches without evidence of human disturbance such as logging and/or fire. We sampled multistemmed adult trees ~1.5 to 2 m height (Figure 1a), located on sunny exposed slopes at mid-elevations of the species local altitudinal distribution, avoiding depressions, ravines or gullies. Cross sections were obtained from one of the multiple stems of the selected living trees and from relict dead wood.

We generated ombrothermic diagrams at each study site (Figure 1c) using a 1° grid resolution ERA Interim product (1979–2018, Dee et al. 2011) obtained from KNMI Climate Explorer (https://climexp.knmi.nl), and CHIRPS data for PP (1981–2018, Funk et al. 2015) obtained from the IRI/LDEO Climate Data Library (https://iridl.ldeo.columbia.edu). CHIRPS data are based both on remote sensing and meteorological stations. CHIRPS is a gridded product with limited time span (1981–2018), but high spatial resolution (0.05 × 0.05°) and it is considered a very high-quality product for precipitation for the tropical regions. Although no meteorological data were available on the study sites, CHIRPS data are a good choice to represent the features of each site in our gradient in a reliable way for the recent decades. Most PP in the Altiplano falls during the austral summer months, with 80–90% concentrated from December to March consistent with the South American Summer Monsoon circulation (Garreaud et al. 2003, Vuille and Keimig 2004). This agrees with January being the rainiest month at our four study sites (Figure 1c). The north-south PP gradient, along which the sites are distributed, ranges from ~300 mm year^{-1} of mean total annual precipitation at the GUA and FSA sites, to ~200 mm year^{-1} at the IRR and UTU sites (Figure 1c).

Table 1. *Polylepis tarapacana* sites for tree-ring width index (RWI), $\delta^{13}C$ and $\delta^{18}O$ isotope chronologies.

Site	Code	Country	Latitude (South)	Longitude (West)	Elevation (m a.s.l.)	Slope	*N* trees RWI	*N* trees stable isotopes
Guallatiri	GUA	Chile	18°28′	69°04′	4600	SW	44	5
Frente Sabaya	FSA	Bolivia	19°06′	68°27′	4550	E-SE	49	5
Irruputuncu	IRR	Chile	20°43′	68°34′	4400	W	60	5
Uturunco	UTU	Bolivia	22°18′	67°14′	4650	E-NE	40	5

Table 2. Statistics for RWI, $\delta^{18}O$ and $\delta^{13}C_c$ chronologies.

Site code	Period RWI $\geq$ 5 series	Average $\pm$ SE raw ring width (mm)	Mean r_{site} RWI	EPS RWI	Period $\delta^{18}O$ and $\delta^{13}C_c$	Mean r_{site} $\delta^{18}O$	EPS $\delta^{18}O$	Mean r_{site} $\delta^{13}C_c$	EPS $\delta^{13}C_c$
GUA	1395–2015	0.53 $\pm$ 0.02	0.43	0.97	1950–2015	0.77	0.94	0.15	0.47
FSA	1463–2008	0.58 $\pm$ 0.03	0.36	0.92	1950–2008	0.86	0.97	0.30	0.68
IRR	1348–2009	0.55 $\pm$ 0.01	0.31	0.97	1950–2008	0.58	0.87	0.19	0.53
UTU	1430–2013	0.44 $\pm$ 0.01	0.69	0.94	1950–2013	0.69	0.92	0.34	0.72

Longer climate records were used to assess the relationships between the tree-ring chronologies and climate. Monthly regional PP and T records from 1950 to 2008 were obtained averaging anomalies from 32 and 7 meteorological stations, respectively (Figure 1b, Table S1 available as Supplementary data at *Tree Physiology* Online). Considering that the spatial variation of air T anomalies over the Altiplano is small (Vuille et al. 2000), we used the four best T series (i.e., less missing data and longer coverage) from a total of seven T weather stations (Table S1 available as Supplementary data at *Tree Physiology* Online). We also compared tree-ring chronologies with a monthly regional self-calibrating Palmer Drought Severity Index (PDSI) (van der Schrier et al. 2013). See Supporting Information Appendix S1 for detailed methods for developing the climate series used.

The ring-width, oxygen and carbon tree-ring chronologies

Ring widths were measured on cross sections from 40 to 60 stems of individual *P. tarapacana* trees (Christie et al. 2009, Morales et al. 2012, Table 2). The raw measurements were transformed into RWI by fitting negative exponential curves to each individual series using dplR (Bunn 2008). This standardization is a relatively conservative method for removing nonclimatic variability from the ring-width series, such as tree age or size trends (Cook et al. 1990).

At each *P. tarapacana* location, we selected five trees to develop the $\delta^{18}O$ and $\delta^{13}C$ individual tree-ring isotopic time series, which were averaged to obtain the site isotopic chronologies from 1950 to the last available year (2008–2015, Table 2). We analyzed individual rings from each tree; therefore, no sample pooling was performed. At the laboratory, wood slices ~2.0–3.0 mm thick were cut from the selected cross sections. Each tree ring was carefully separated using a scalpel under the microscope and the resulting wood was chopped into wood slivers ~2.0–3.0 mm long and 0.5–1.0 mm wide. In this angiosperm species tree rings are small (~0.5 mm, Table 2) and earlywood and latewood are not easily discernible. Therefore, the whole tree ring was used for cellulose extraction. Alpha cellulose was extracted from wood samples, homogenized using an ultrasound bath and freeze-dried, and 200 µg of cellulose from each ring was encapsulated in silver capsules (Andreu-Hayles et al. 2019). The $\delta^{18}O$ and $\delta^{13}C$ ratios were measured at the same time using a dual method approach (see details in Andreu-Hayles et al. 2019), in which cellulose samples were converted to CO gas through high-temperature pyrolysis at 1400 °C using a high-temperature conversion elemental analyzer (TC/EA, Thermo Scientific Finnigan, Bremen, Germany) interfaced with a Thermo Delta V plus mass spectrometer (Thermo Scientific, Waltham, Massachusetts, United States of America) (Gehre and Strauch 2003). We used primary standards IAEA-601 and IAEA-602 for $\delta^{18}O$, and IAEA-C3, IAEA-CH6 for $\delta^{13}C$ (International Atomic Energy Agency, Vienna, Austria) to convert the raw values from the IRMS in δ notation as per mil (‰) in relation to the international materials: the Vienna Standard Mean Ocean Water for $\delta^{18}O$ (VSMOW) and the Vienna Pee Dee Belemnite for $\delta^{13}C$ (VPDB). We also used the secondary standards USGS-54 (United States Geological Survey, Reston, Virginia, United States of America) and Sigma Alpha-Cellulose and Sigma Sucrose (Sigma-Aldrich Chemicals, St Louis, Missouri, United States of America) to check the quality and precision of our extrapolation. The analytical precision of our isotope measurements is $\pm$0.15 for $\delta^{18}O$ and $\pm$ 0.13 for $\delta^{13}C$.

The $\delta^{13}C$ values were corrected ($\delta^{13}C_c$) for the effect of declining atmospheric $\delta^{13}C$ ($\delta^{13}C_a$) due to anthropogenic fossil

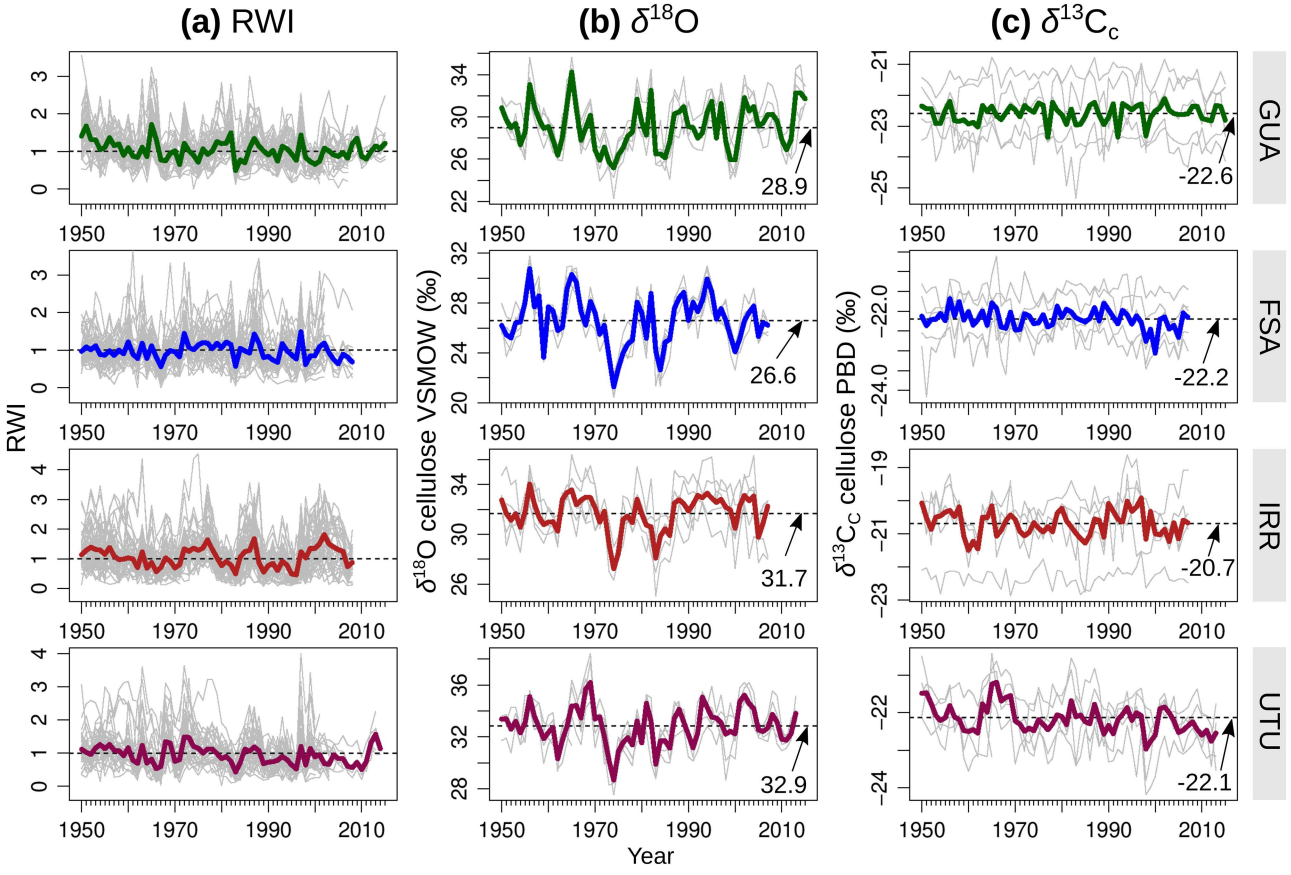

Figure 2. (a) The ring-width index (RWI), (b) oxygen ($\delta^{18}O$) and (c) corrected carbon ($\delta^{13}C_c$) tree-ring chronologies at each site. Individual tree-ring series are represented by gray thin lines, and the site chronologies by thick colored lines. Average values of $\delta^{18}O$ and $\delta^{13}C_c$ for the 1950–2008 common period are shown by horizontal dashed lines.

fuel burning (i.e., the 'Suess Effect', Suess 1955) by subtracting from annual raw measurements the annual changes in the $\delta^{13}C_a$ for the Southern Hemisphere (Leuenberger 2007), linearly interpolated over 2007–2015.

The RWI, $\delta^{18}O$ and $\delta^{13}C_c$ individual tree time series available at each site were averaged to generate the RWI, $\delta^{18}O$ and $\delta^{13}C_c$ site chronologies, respectively (Figure 2). For each site chronology, mean values of raw ring width (Table 2), $\delta^{18}O$ and $\delta^{13}C_c$ and their standard errors were calculated for the common period 1950–2008 (Figure 3a). For each proxy, the agreement among tree-ring series was represented by the mean Pearson correlation coefficients between individual trees within sites (mean r_{site}, Table 2) and between site chronologies (mean $r_{regional}$, Figure S2 available as Supplementary data at *Tree Physiology* Online). At each site, correlations between RWI, $\delta^{18}O$ and $\delta^{13}C_c$ chronologies were also calculated (Figure 3b). The quality of the chronologies was measured by the Expressed Population Signal (EPS, Wigley et al. 1984). The EPS represents the total common signal in a chronology in relation to an infinitely replicated chronology (Wigley et al. 1984, Cook et al. 1990). EPS values close to or >0.85 indicate that the number of samples that integrate the chronology in a given period represents a significant amount of the theoretical signal present in an infinitely replicated chronology.

In order to obtain the CO_2 concentration within intercellular spaces (C_i) (Figure S3 available as Supplementary data at *Tree Physiology* Online), the tree-ring cellulose $\delta^{13}C$ ($\delta^{13}C_{cell}$) and the atmospheric $\delta^{13}C_a$ isotopic values were used following Francey and Farquhar (1982):

$$C_i = C_a^* \left(\delta^{13}C_{cell} - \delta^{13}C_a + a\right) / (a - b), \quad (1)$$

where C_a is the atmospheric CO_2 concentration and a (4.4‰) and b (27‰) represent the fractionation associated with diffusion of CO_2 through stomata and the fractionation associated with carbon fixation, respectively.

Relationships between climate and tree-ring parameters

Pearson correlation coefficients were performed between the RWI, $\delta^{18}O$ and $\delta^{13}C_c$ tree-ring chronologies and the monthly regional T and PP anomalies from August of the previous year to May of the current year (Figures 4 and 5). The analyses were conducted using the R package *treeclim* (Zang and Biondi 2015), and the significance of the correlation coefficients

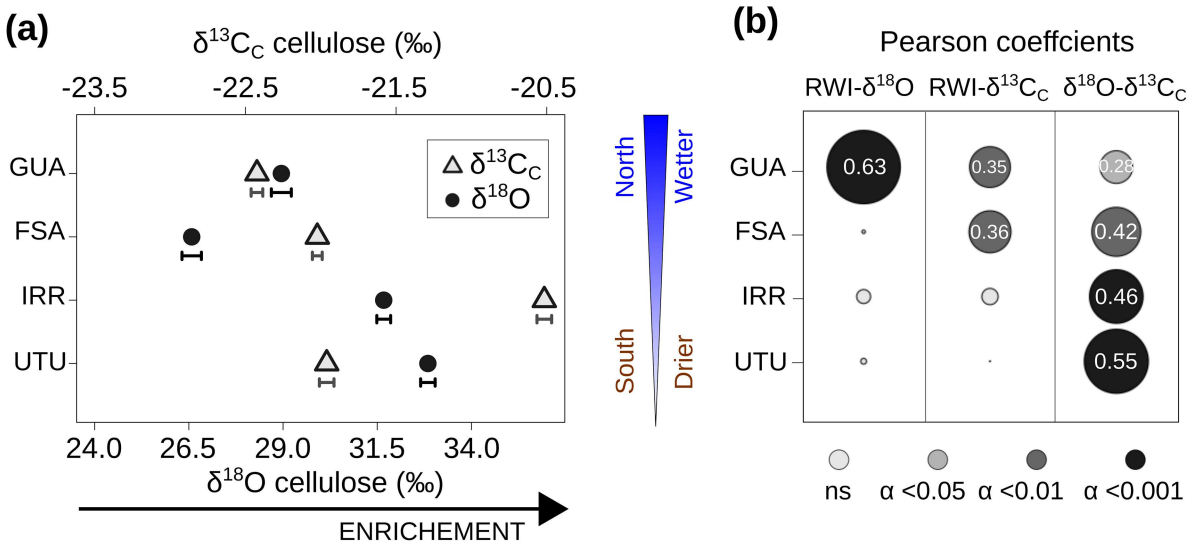

Figure 3. (a) Mean values of $\delta^{18}O$ (black circles) and $\delta^{13}C_c$ (gray triangles) for each site chronology for the common period 1950–2008. The standard error of the mean is shown as horizontal bars below each value. (b) Pearson correlation coefficients among tree-ring width index (RWI), $\delta^{18}O$ and $\delta^{13}C_c$ at each site for the common period 1950–2008. Circle size and color intensity indicate absolute values and significance levels of the correlations, respectively.

was assessed by stationary bootstrapped confidence intervals (Biondi and Waikul 2004).

Since PP and T in the Altiplano are anticorrelated on seasonal and interannual scales, particularly during the growing season (Figure S1 available as Supplementary data at *Tree Physiology* Online) (Vuille and Keimig 2004), partial correlations that remove the influence of the covariance between these two variables were computed. The partial correlation coefficients between climate and the tree-ring chronologies were estimated using *seascorr* function from *treeclim* (Meko et al. 2011, Zang and Biondi 2015). The partial correlations between climate and the tree-ring chronology were estimated as follows:

$$r_{PP.Cr|T} = \left[r_{PP.Cr} - r^{*}_{T.PP} r_{T.Cr}\right] / \left[\text{sqrt}\left(1 - r^{2}_{T.PP}\right)^{*} \text{sqrt}\left(1 - r^{2}_{T.Cr}\right)\right] \quad (2)$$

$$r_{T.Cr|PP} = \left[r_{T.Cr} - r_{T.PP}{}^{*} r_{PP.Cr}\right] / \left[\text{sqrt}\left(1 - r^{2}_{T.PP}\right)^{*} \text{sqrt}\left(1 - r^{2}_{PP.Cr}\right)\right] \quad (3)$$

in which $r_{PP.Cr|T}$ ($r_{T.Cr|PP}$) is the partial correlations between PP (T) and the tree-ring chronology without the influence of T (PP); $r_{T.Cr}$ and $r_{PP.Cr}$ are Pearson correlation coefficients between the tree-ring chronology and T and PP, respectively; and $r_{T.PP}$ is the Pearson correlation coefficient between T and PP. Note that the absolute values of partial correlation coefficients are lower than the ones of Pearson correlation coefficients by design. Partial correlations were calculated month-by-month from August of the previous year to May of the current year (Figures 4 and 5). Based on the significance of Pearson correlations between the RWI chronology and climate, we defined the growing season from November to March and calculated partial correlations for the previous and current growing seasons (Figure 6). Pearson correlations were also calculated between the tree-ring chronologies and PDSI. All correlations were performed for the common period 1950–2008.

Years with extremely narrow (25th percentile) and wide rings (75th percentile) were selected over the common period 1950–2008 and the associated climate conditions and isotopic values were determined. To eliminate the interdependence of current- and prior-year in tree rings in this analysis, we selected the extreme years from residual chronologies (Figure S4 available as Supplementary data at *Tree Physiology* Online). The residual chronologies were obtained by applying an autoregressive model (Cook 1985) that removes the intrinsic internal autocorrelation of the RWI data while enhancing high-frequency variability. Monthly PP and T departures during the extreme years were averaged for the growing season. Statistical differences between the narrowest and widest rings were evaluated using Kolmogorov-Smirnov tests for climate conditions and isotopic values. All analyses were performed using R (R Development Core Team 2020).

Results

The ring-width, oxygen and carbon tree-ring chronologies

The width of the tree rings was around 0.5 mm in average for all four sites (Table 2). The mean values of the $\delta^{18}O$ and $\delta^{13}C_c$ chronologies for the common period (1950–2008) showed differences along the latitudinal gradient (Figure 3a). More enriched mean $\delta^{18}O$ values were found at the southern sites (31.7‰ for IRR and 32.9‰ for UTU) than at the northern sites (28.9‰ and 26.6‰ at GUA and FSA, respectively). The mean $\delta^{13}C_c$ values for all the sites (Figure 3a) were around

−22‰ (C_i = 170 mmol CO_2 mol air^{-1}, Figure S3a available as Supplementary data at *Tree Physiology* Online), only higher for IRR reaching −20.7‰ (C_i = 150 mmol CO_2 mol air^{-1}). A proportional rate of increase between C_i and C_a (constant C_i/C_a) was observed for the four sites in the last 60 years (Figure S3a available as Supplementary data at *Tree Physiology* Online).

The agreement among individual trees at each site was assessed by the mean Pearson correlation coefficients (mean r_{site}) and the EPS (Table 2). The RWI mean r_{site} ranged from 0.31 to 0.69, the $\delta^{18}O$ mean r_{site} ranged from 0.58 to 0.86, and the $\delta^{13}C_c$ mean r_{site} had lower values ranging from 0.15 to 0.34 (Table 2). Based on EPS and mean r_{site}, all the $\delta^{18}O$ chronologies, composed by five trees, shared almost as much common variance as the RWI chronologies, composed by 44 to 60 trees, demonstrating an adequate level of sample replication in the $\delta^{18}O$ chronologies.

When we compared the regional coherence among chronologies for each proxy along the gradient, the results were similar to those found within site. The RWI mean $r_{regional}$ was 0.44 (range = 0.17–0.58), the $\delta^{18}O$ mean $r_{regional}$ was 0.70 (range = 0.62–0.77) and the $\delta^{13}C_c$ mean $r_{regional}$ was 0.33 (range = 0.20–0.41) (Figure S2 available as Supplementary data at *Tree Physiology* Online). Hence, overall common local and regional interannual variability was highest for oxygen isotope chronologies.

Within each site, the $\delta^{18}O$ and $\delta^{13}C_c$ chronologies shared common variance as indicated by the positive and significant correlation coefficients (Figure 3b). While the southernmost site UTU showed the highest Pearson correlation coefficients between $\delta^{18}O$ and $\delta^{13}C_c$ chronologies (r = 0.55), the northernmost site GUA showed the lowest (r = 0.28) (Figure 3b, Figure S5 available as Supplementary data at *Tree Physiology* Online). Correlations between RWI and $\delta^{18}O$ were significant only at GUA and those between RWI and $\delta^{13}C_c$ were significant only at the two northern sites (Figure 3b).

Relationship between ring-width, oxygen and carbon tree-ring chronologies and precipitation

Figure 4 shows the monthly Pearson correlation coefficients between PP and the RWI, $\delta^{18}O$ and $\delta^{13}C_c$ chronologies for the four study sites along with the partial correlation coefficients with PP after removing PP covariability with T. The northern GUA and FSA RWI chronologies showed negative correlation coefficients with current growing-season PP during January, February and March (JFM), the rainiest months. These coefficients were significant only for GUA (vertical solid lines in Figure 4a). However, after removing the covariance with T, the negative association between current growing-season PP and RWI at GUA was not significant (bars in Figure 4a). By contrast, all RWI chronologies showed consistently positive relationships with previous-year PP, with distinct levels of significance from previous November to previous March and increasing partial correlation coefficients toward the south (Figures 4a and 6a). The higher correlation values at the two southern sites indicated that RWI was mostly favored by previous growing-season PP (Figure 6a) than current PP (Figure 6b), as well as more humid conditions in both previous and current growing seasons as indicated by positive and significant correlations between RWI and PDSI (Figure 6e and f).

The $\delta^{18}O$ chronologies showed significant and negative relationships with PP during current JFM at all sites (Figure 4b). Correlation coefficients were approximately −0.6, particularly strong in January, and also significant for partial correlations. The strength of the negative relationship between $\delta^{18}O$ chronologies and current growing-season moisture conditions (PP and PDSI) decreased from north to south (Figure 6b and f). Weaker negative correlations were also found between $\delta^{18}O$ and previous-growing season PP except for UTU (Figure 4a), albeit nonsignificant for any site from previous November to March (Figure 6a).

The four $\delta^{13}C_c$ chronologies also showed negative relationships with PP during current JFM (Figure 4c). Negative and significant correlations between $\delta^{13}C_c$ and previous spring and prior autumn PP were also found for both Pearson and partial correlations in three of the sites. Positive correlations were also found between $\delta^{13}C_c$ and previous November to December PP for GUA and FSA (Figure 4c).

Relationship between ring-width, oxygen and carbon tree-ring chronologies and temperature

After removing the covariance between PP and T, the GUA RWI chronology showed the highest and longest-lasting positive relationship with current-year T, indicated by significant correlation coefficients from October to May with the highest value in January (r = 0.7, Figure 5a). For GUA RWI, current growing-season T had the highest partial correlation coefficients among previous and current growing-season climate variables (GUA RWI in Figure 6d versus GUA RWI in Figure 6a–c,e,f). The FSA RWI chronology showed significant relationships with current growing-season T during January and February, albeit lower coefficients than for GUA RWI (Figure 5a). By contrast, the southernmost IRR and UTU RWI chronologies did not show any significant relationship with current growing-season T, but they did correlate negatively with T from previous October to prior August (Figure 5a). Similar results were obtained using T data from seven stations (Figure S6 available as Supplementary data at *Tree Physiology* Online), showing that this lack of sensitivity of growth to current growing-season T in the southern sites was not due to the use of northern weather stations.

In concordance, when removing autocorrelation, the widest rings in the northern sites were produced during warm and dry conditions in the current growing season, whereas the widest rings in the southern sites corresponded to wet and cold conditions in the prior growing season (Figure S7a available as

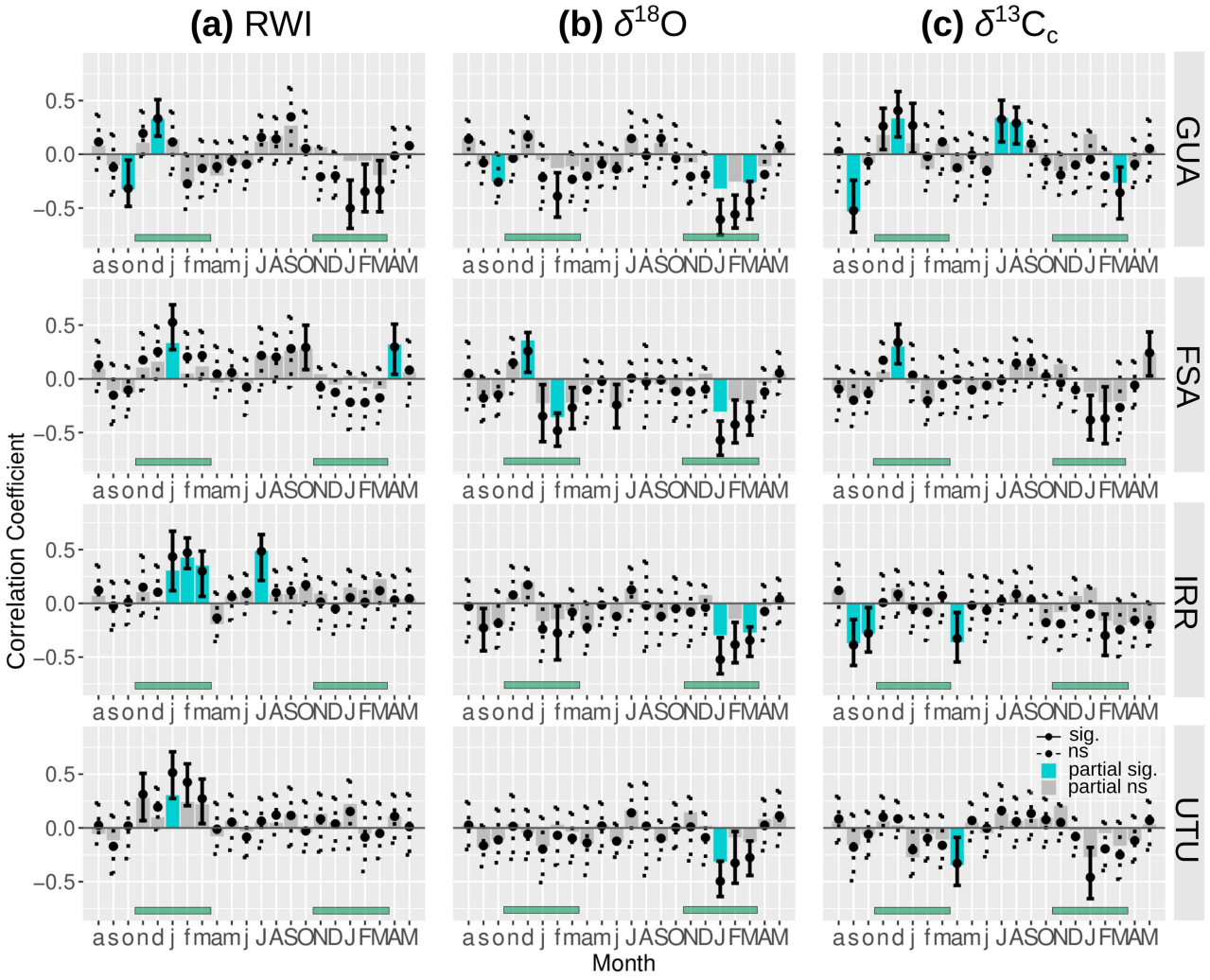

Figure 4. Correlation coefficients between monthly regional precipitation and (a) ring-width index (RWI), (b) $\delta^{18}O$ and (c) $\delta^{13}C_c$ tree-ring chronologies from August prior-year (lowercase) to May current-year (uppercase). Vertical lines represent bootstrap monthly correlations with solid lines indicating significant (sig.) and dashed lines nonsignificant correlations (ns). Bars represent partial monthly correlations where the relationship of each tree-ring variable (RWI, $\delta^{18}O$, $\delta^{13}C_c$) and precipitation was computed after removing the covariability between precipitation and temperature. Colored bars indicate significant coefficients (partial sig.) and gray bars nonsignificant partial correlations (partial ns). Duration of the growing season is indicated by a green horizontal line.

Supplementary data at *Tree Physiology* Online). The widest rings showed more enriched (higher) values of $\delta^{18}O$ at GUA and more enriched $\delta^{13}C_c$ at the northern-wetter GUA and FSA sites than the narrowest rings (Figure S7b available as Supplementary data at *Tree Physiology* Online).

All the $\delta^{18}O$ chronologies exhibited consistent and positive relationships with current growing-season T from October to May, reaching the highest values in January ($r \sim 0.7$; Figure 5b). Similar to the relationships with PP, the northern $\delta^{18}O$ chronologies showed higher correlations with current growing-season T than the southern $\delta^{18}O$ chronologies (Figure 6d). Note that correlation coefficients with T were also positive for prior-growing season and stronger in the northern sites, albeit not significant for partial correlations (Figures 5b and 6d).

For $\delta^{13}C_c$ chronologies, we also found positive relationships with current growing-season T at all sites (Figure 5c), but the correlation coefficients were lower than between the $\delta^{18}O$ chronologies and current growing-season T (Figure 5b). The $\delta^{13}C_c$ chronologies showed significantly higher coefficients with current November–March PDSI at the southern-drier sites (Figure 6f).

Discussion

A future reduction in the spatial distribution of *P. tarapacana* woodlands is predicted by the end of the 21th century associated to the projected warming and drying trends for the South American Altiplano (Cuyckens et al. 2016).

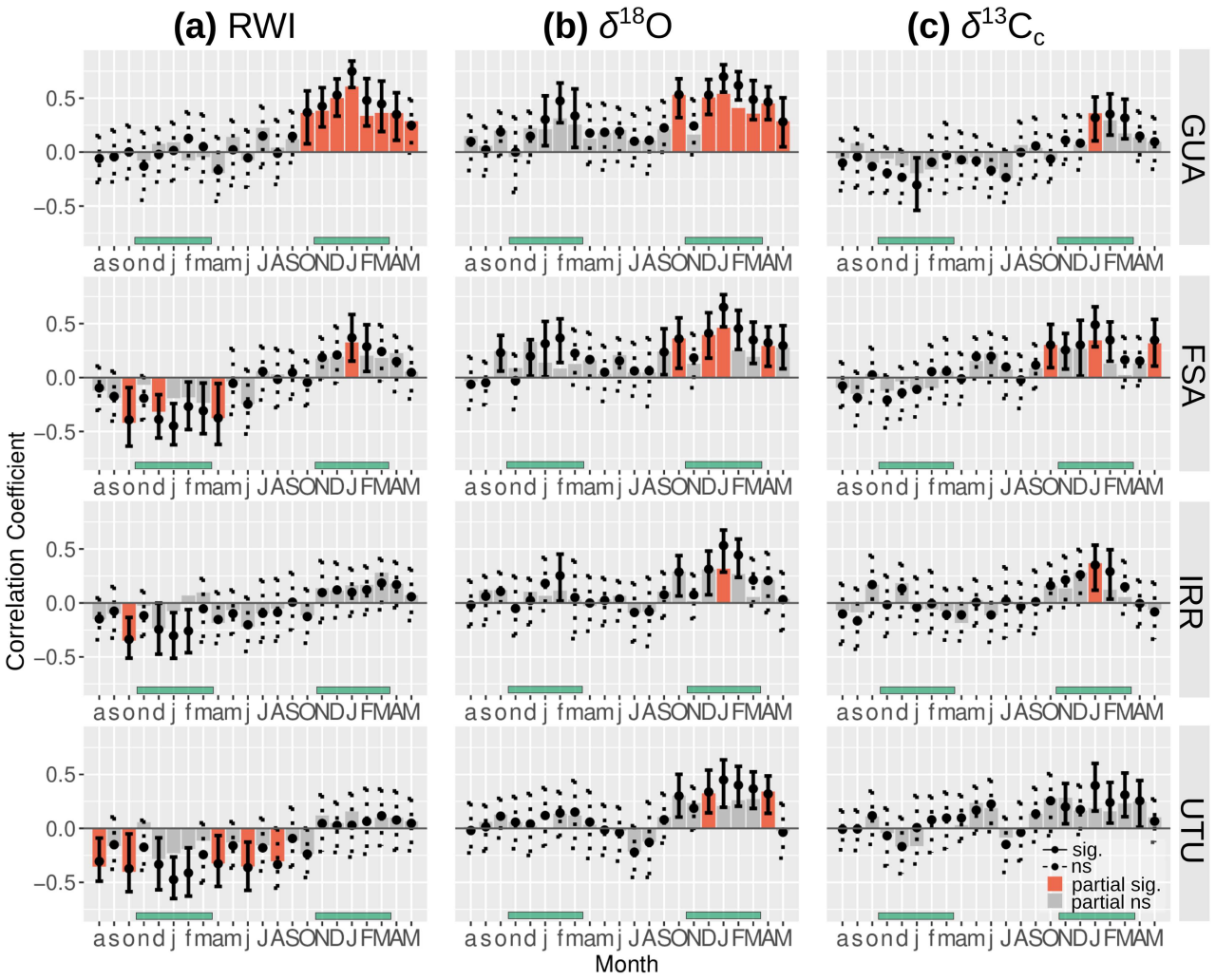

Figure 5. Correlation coefficients between monthly regional temperature and (a) ring-width index (RWI), (b) $\delta^{18}O$ and (c) $\delta^{13}C_c$ tree-ring chronologies from August prior-year (lowercase) to May current-year (uppercase). Vertical lines represent bootstrap monthly correlations with solid lines indicating significant (sig.) and dashed lines nonsignificant correlations (ns). Bars represent partial monthly correlations where the relationship of each tree-ring variable (RWI, $\delta^{18}O$, $\delta^{13}C_c$) and temperature was computed after removing the covariability between temperature and precipitation. Colored bars indicate significant coefficients (partial sig.) and gray bars nonsignificant partial correlations (partial ns). Duration of the growing season is indicated by a green horizontal line.

To better understand *P. tarapacana* ecophysiology and its potential future behavior under climate change, we tested the relationships between *P. tarapacana* radial growth, $\delta^{18}O$ and $\delta^{13}C$ stable isotope chronologies and climate along a latitudinal aridity gradient. As discussed below, the climate responses estimated using *P. tarapacana* ring-width and stable isotope chronologies suggest that for these high-elevation trees: (i) radial growth (carbon sink) can be limited by precipitation or temperature depending on site location along the aridity gradient; (ii) current growing-season climatic factors influence stable isotopes (carbon source) similarly at all the sites; (iii) stomatal conductance appears as the dominant mechanism that controls intercellular CO_2 concentration at all sites showing higher strength when aridity increases; (iv) carbon sink and carbon source processes seem to be coupled in the northern-wetter sites due to similar and synchronous climate sensitivity, while they may be decoupled at southern-drier sites due to different and asynchronous sensitivity to climate conditions.

Contrasting climate factors limiting radial growth along the aridity gradient

Turgor pressure, which depends on available moisture, and T have to reach certain thresholds to trigger xylem cell division, expansion and differentiation (Muller et al. 2011, Körner 2015). In temperate and boreal forests, annual tree rings are well defined due to the dormancy of the vascular cambium as T decreases during winter (Begum et al. 2018). Conversely, in tropical regions, T is more uniform all year around and the formation of annual ring boundaries is usually related to

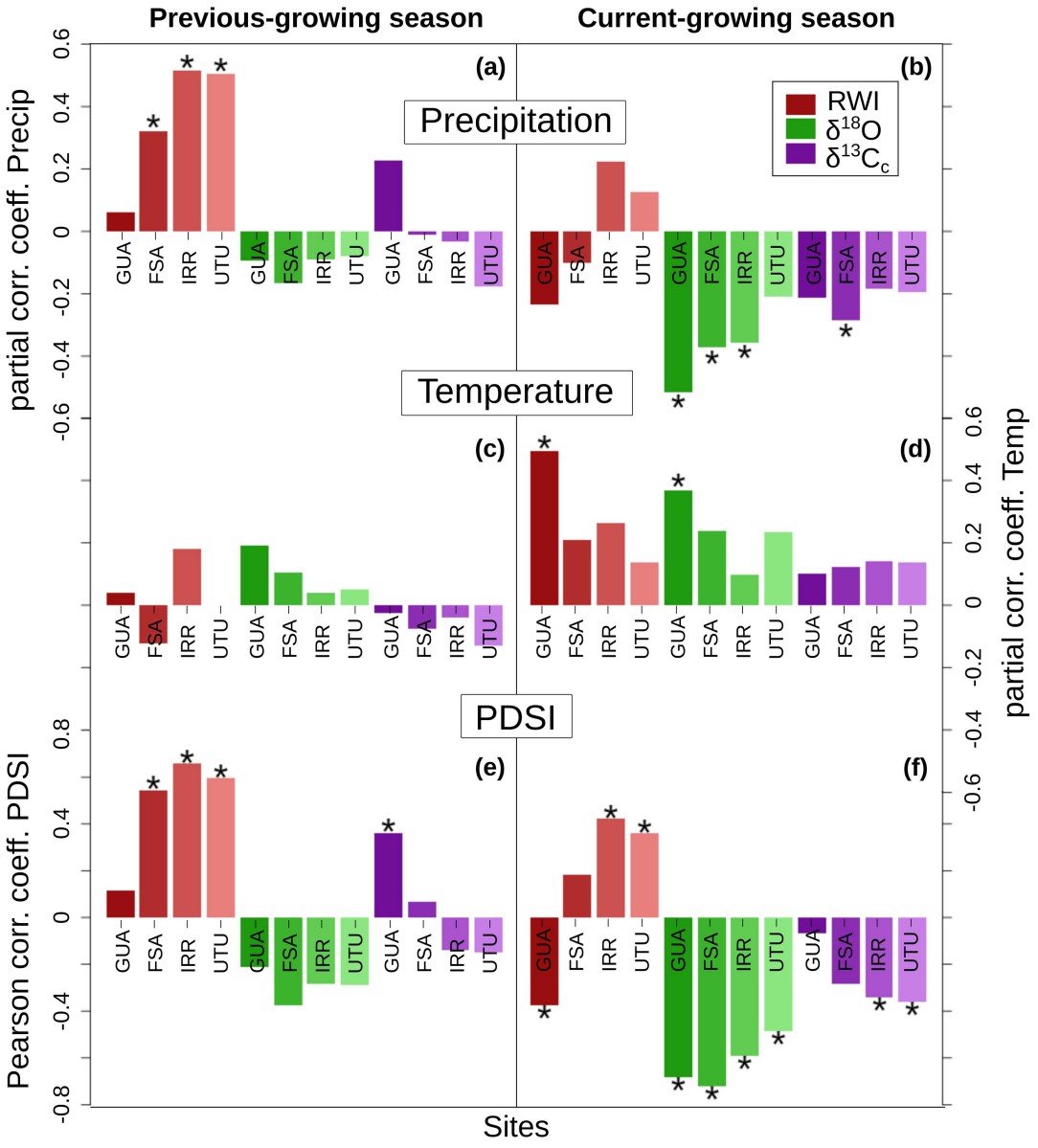

Figure 6. Correlation coefficients between the tree-ring width index (RWI), $\delta^{18}O$ and $\delta^{13}C_c$ chronologies and previous and current growing-season climate from November to March at the four study sites. For (a, b) precipitation and (c, d) temperature bars represent partial correlations that remove covariance between both climate variables, while correlations with (e, f) palmer drought severity index (PDSI) are simple Pearson correlations. Statistically significant correlations are indicated with stars (alpha = 0.05).

a dry season (Rahman et al. 2019). In the high-elevation mountains in the Central Andes, more than 80% annual rainfall is concentrated in the austral summer (December to March), while there is almost no precipitation during austral winter. Minimum T is higher during summer coincident with this wet season (see Figure 1 in García-Plazaola et al. 2015). Therefore, the well-defined annual tree rings of *P. tarapacana,* characterized by vessels arranged in semicircular porosity (Requena-Rojas and Taquire Arroyo 2019), may be modulated by seasonal changes in both PP and T. Correlations between RWI and climate provide information on the environmental factors controlling interannual variations in stem growth. Our results using partial correlations demonstrated the independent influence of both PP and T on radial growth. This agrees with findings in other high-elevation semiarid areas where tree-ring formation of *Juniperus przewalskii* also depended on both PP and T (Ren et al. 2018).

In order to facilitate the discussion on the three tree-ring proxies and the climate relationships along the aridity gradient, we summarized in Figure 7 the 24 plots shown in Figures 4 and 5. We found that RWI was positively correlated with PP and negatively correlated with T during the previous growing season, particularly at the driest sites at the southern portion of our gradient (Figure 7). This is consistent with previous studies showing *P. tarapacana* ring-width positively correlated with

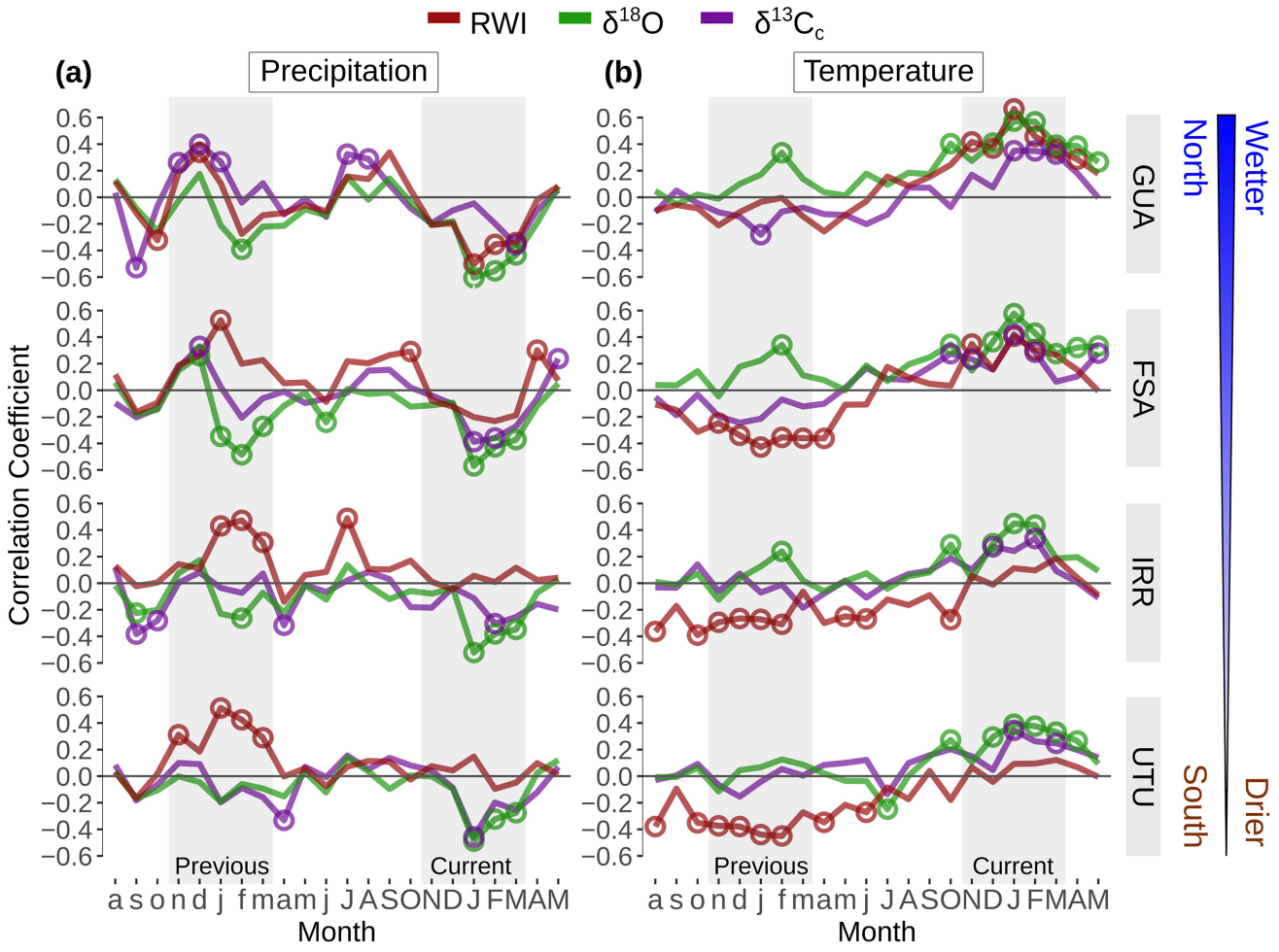

Figure 7. Summary of Pearson correlation coefficients between monthly regional (a) precipitation and (b) temperature and ring-width index (RWI), $\delta^{18}O$ and $\delta^{13}C_c$ tree-ring chronologies from August prior-year (lowercase) to May current-year (uppercase). Circles represent significant correlations and gray vertical shading highlight previous- and current-growing seasons.

previous growing-season water availability (Argollo et al. 2004, Morales et al. 2004, Christie et al. 2009, Soliz et al. 2009).

At the southern sites, RWI also seems to be favored by wetter conditions during the current growing season as suggested by the significant and positive response to the drought index PDSI (Figure 6f). In this arid high-elevation environment, intense solar irradiance combined with low cloud cover causes daily maximum T to reach 25 °C in austral spring and summer (Hoch and Körner 2005). High daytime T likely exacerbates both soil water evaporation and evapotranspiration, increasing water deficit and limiting radial growth. Under this scenario, we would expect a strong negative influence of current growing-season T on radial growth. Instead, we found a positive relationship with current growing-season T, albeit nonsignificant at these southern sites (Figure 6d, Figure 7b). The positive effect of T on xylogenesis (Rossi et al. 2008) in this cold environment may explain this pattern. In other words, T influence on ring width could be simultaneously negative (indirectly through desiccation at a daily scale) and positive (directly regulating xylogenesis at seasonal scale, which can be particularly relevant for the onset of growth). These responses can potentially mask each other, explaining the lack of a current growing-season T signal in the southern-drier sites.

Climate sensitivity is different at the northern-wetter sites, where current growing-season T significantly limits tree growth (Figure 7b). To test if this was true for a wider geographical region, we used 14 ring-width chronologies of *P. tarapacana* from Soliz et al. (2009) (Figure 8a). Based on principal component analysis, Soliz et al. (2009) found shared variance between ring-width chronologies located below and above 20° S. Taking into account this latitudinal threshold, we correlated our regional T series with the 14 residual ring-width chronologies from Soliz et al. (2009). Consistent with the RWI climate sensitivity observed in our four study sites, there was a higher positive influence of current growing-season T on radial growth at the northern-wetter sites of this network of RWI chronologies (Figure 8b). Conversely, previous growing-season moisture moisture (i.e., negative correlation with T) favored stem growth at the southern-drier sites along the network (Figure 8b). These correlation patterns highlight the distinct

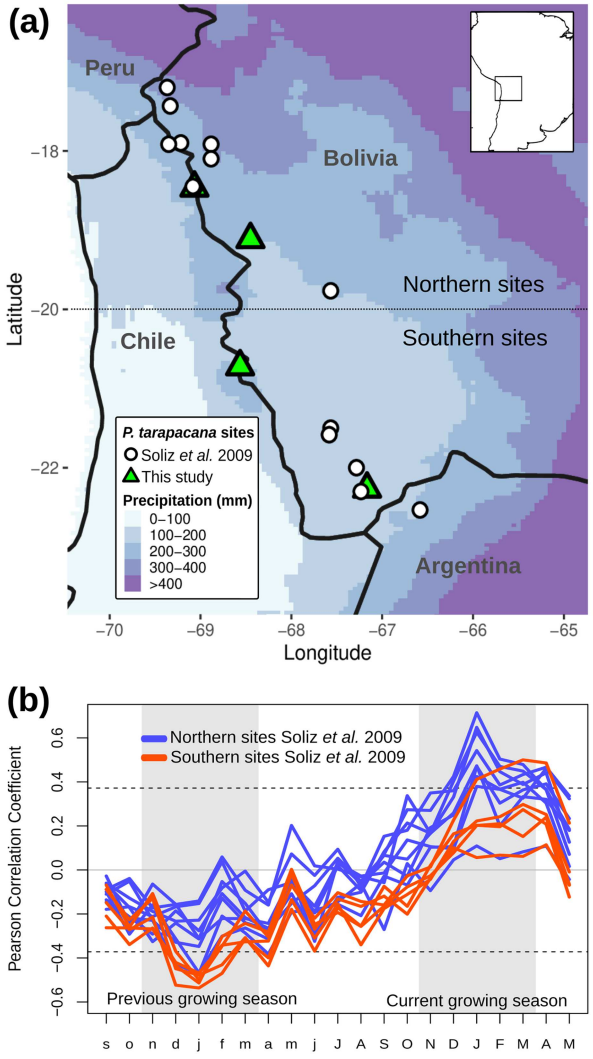

Figure 8. (a) Network of *Polylepis tarapacana* ring-width chronologies from this study (green triangles) and from Soliz et al. (2009) (white circles). Background colors represent mean total annual precipitation for the period 1981–2018 from CHIRPS data set; note the north-south aridity gradient. (b) Correlation coefficients between the residual ring-width chronologies from each of the 14 *Polylepis tarapacana* chronologies and mean monthly regional temperatures. We divided the total number of chronologies located north of 20°S (northern chronologies) and south of 20°S (southern chronologies). The criterion for defining 20°S was based on the results of the principal component analysis performed by Soliz et al. (2009). Dashed horizontal lines represent significance level (alpha = 0.01).

climate sensitivity between northern-wetter and southern-drier sites along the network and may explain the spatial variability observed by Soliz et al. (2009).

At similar elevations to our study sites but with higher annual PP (around 900 mm), *Polylepis rodolfo-vasquezii*, a species growing in the Peruvian highlands, shows a strong positive relationship with current growing-season T (Requena-Rojas et al. 2020). Together with our results, this indicates that current growing-season T controls growth at high elevations to the extent as water needs are met. Our findings suggest that wetter sites of *P. tarapacana* behave like T-limited treeline sites in less arid regions, where higher T enhances meristematic activity (Shi et al. 2008). However, if low-water availability periods are expected to be more frequent and persistent in a more arid and warmer Altiplano (Minvielle and Garreaud 2011, Thibeault et al. 2012, Neukom et al. 2015), northern-wetter sites could start behaving as PP-limited treelines, similar to the present-day southern more arid sites.

Insights from oxygen and carbon stable isotope signatures in tree rings

The mean values of tree-ring $\delta^{13}C_c$ measured in this study were around −22 and −20‰ (Figure 3a), which are in the 'enriched' end for C3 plants and even reaching C4 plant values (site IRR) (O'Leary 1988). These values are higher than those in most species consistent with lower discrimination rates observed in higher elevation habitats (Körner et al. 1988). Mean $\delta^{13}C_c$ values of approximately−20.5‰ were reported for *Juniperus tibetica* and *Picea balfouriana* tree rings in the Tibetan Plateau at similar elevations than our study sites (Grießinger et al. 2019). Leaf measurement of $\delta^{13}C$ in *P. tarapacana* has yielded values from −23 to −26‰ (Macek et al. 2009), which increased with elevation (Hoch and Körner 2005). The observed difference between these more depleted $\delta^{13}C_c$ values in leaves (e.g., −23 to −26‰, Macek et al. 2009) and our tree-ring $\delta^{13}C_c$ values (approximately −22 to −20‰) in *P. tarapacana* is expected based on carbon fractionation processes that favor ^{12}C during phloem transport, starch metabolism and trunk respiration, with a remaining more enriched $\delta^{13}C$ to be use for cellulose production (Gessler et al. 2014).

We found that current growing-season PP and T influenced both $\delta^{18}O$ and $\delta^{13}C_c$ chronologies at the four study sites. Unlike $\delta^{18}O$, $\delta^{13}C_c$ data exhibited lower correlations and higher variability between trees. Individual trees or stems may have specific carbohydrate allocation patterns and/or priorities that may dilute the common signal. Despite this, $\delta^{13}C_c$ chronologies showed shared variance both within and among sites (Table 2, Figure S2 available as Supplementary data at *Tree Physiology* Online), indicating a common environmental factor influencing $\delta^{13}C$ values at local and regional scales. For future analyses, we recommend increasing tree replication for $\delta^{13}C$ to improve the chronologies and potentially enhance this climate signal.

The $\delta^{18}O$ values had a strong PP signal during current JFM, shared between trees within and across the four sites. This suggests that the dominant air masses bringing rain at the four sites have a common origin in the tropical Atlantic Ocean and the Amazon Basin, likely related to the South American Summer Monsoon variability (Vuille et al. 2003). Therefore, the $\delta^{18}O$ signal imprinted in tree rings have a great potential to reconstruct hydroclimatic variability in this region.

According to Rayleigh distillation (Dansgaard 1964), $\delta^{18}O$ in rainfall should be more depleted with increasing distance

from the source water, and more depleted tree-ring $\delta^{18}O$ values would be expected toward the south. However, we found more enriched tree-ring $\delta^{18}O$ in the southern sites (Figure 3a). Because southern sites are drier, higher evaporation of soil water and lower stomatal conductance could explain the observed enriched tree-ring $\delta^{18}O$ values. Although most of the local source water comes from the northeast as mentioned above, the contribution of water vapor with more enriched $\delta^{18}O$ signatures coming from other regions could be another factor to consider (Samuels-Crow et al. 2014).

Stomatal conductance as the primary mechanism controlling intercellular CO_2 concentration

A significant and positive relation between $\delta^{18}O$ and $\delta^{13}C_c$ can reflect a strong control of the isotopic composition of both oxygen and carbon by the stomatal conductance to water vapor (g_s). This postulate is the basis of the dual isotope model (Scheidegger et al. 2000, Grams et al. 2007). At all the sites we found such positive and significant relationships between $\delta^{13}C_c$ and $\delta^{18}O$ (Figure 3b, Figure S5 available as Supplementary data at *Tree Physiology* Online). However, an underlying assumption of the dual isotope model is that source water $\delta^{18}O$ should be invariant so that the majority of $\delta^{18}O$ variation is driven by evaporative enrichment, allowing the interpretation of the $\delta^{18}O$–$\delta^{13}C$ correlation in terms of g_s. While the absence of a relationship between $\delta^{13}C_c$ and $\delta^{18}O$ may not be interpretable (because $\delta^{18}O$ variations may be controlled primarily by source variation obscuring the stomatal effect), stomatal control is the principal mechanism that could explain a strong relation between the two ratios. Therefore, the positive relations we observed between $\delta^{13}C_c$ and $\delta^{18}O$ are consistent with a control of their variations by the evaporative conditions through the modification of the g_s. A corollary to this conclusion is that the net assimilation rate (A_N) may only be a second-order control on $\delta^{13}C_c$ in this environment. Accordingly, the observed increase in iWUE (Figure S3b available as Supplementary data at *Tree Physiology* Online), known to be proportional to A_N/g_s, is consistent with a limited or no increase in A_N and a decrease in g_s.

At the four sites, we observed a constant ratio C_i/C_a (Figure S3a available as Supplementary data at *Tree Physiology* Online). Through stomatal regulation, plants may keep similar rate of increase in C_i than the increase in C_a, which is the most common response observed for in situ studies across the world (Saurer et al. 2004, Frank et al. 2015). This agrees with the least-cost optimality hypothesis, which predicts that leaves minimize the summed costs of transpiration and carboxylation and tend to keep C_i/C_a constant (Wright et al. 2003, Prentice et al. 2014, Lavergne et al. 2020). Overall, our results and the known limitation that VPD exerts on *P. tarapacana* carbon assimilation at hourly and daily scales (García-Plazaola et al. 2015) indicate that g_s is likely the dominant factor controlling the intercellular concentration of CO_2.

The negative (positive) relationship between $\delta^{13}C_c$ and current growing-season PP (T) found along the gradient is consistent with a $\delta^{13}C_c$ enrichment due to a reduction of the g_s when aridity increases. In addition, our southern-drier sites showed significant $\delta^{13}C_c$ enrichment during dry years (lower PDSI, Figure 6f) and higher correlation coefficients between $\delta^{18}O$ and $\delta^{13}C_c$ chronologies compared with northern sites (Figure 3b, Figure S5 available as Supplementary data at *Tree Physiology* Online). These results suggest increasing strength of stomatal regulation in the southern arid sites. The lower g_s measured in *P. tarapacana* at the Sajama Volcano (18°7′S and 68°57′W, 4300 m a.s.l.) during the dry-cold season in comparison with the wet-warm season (Garcia-Nuñez et al. 2004) agrees with the higher stomatal regulation when aridity increases in these high-elevation evergreen forests.

Linking carbon sink and carbon source processes

At the northern sites, we found similar and synchronous climate response between radial growth and stable isotopes (i.e., higher current growing-season T favors RWI and leads to enriched $\delta^{18}O$ and $\delta^{13}C_c$) (Figure 7). Higher T may enhance meristematic activity leading to wider rings, in line with the sink limitation hypothesis (Körner 2003, 2015, Hoch and Körner 2005, Palacio et al. 2014). In this scenario, the positive and significant relationship between RWI and $\delta^{13}C_c$ observed in the northern sites (Figure 3b) may be due to a higher chance of collecting a stomata-driven enriched $\delta^{13}C$ when wider rings are formed. Indeed, at the northern sites, the widest rings were significantly more enriched in $\delta^{13}C_c$ and associated with higher T than the narrowest rings (Figure S7 available as Supplementary data at *Tree Physiology* Online). These results suggest a coupling between carbon sink and carbon source processes at the northern sites. By contrast, in the southern-drier sites, the climate response for radial growth and tree-ring isotopes was opposite and lagged in time. While wider rings occurred when the previous year was wet and cold (higher water availability), more enriched $\delta^{18}O$ and $\delta^{13}C_c$ were associated with warmer and drier current growing-season climate (Figure 7). This opposite and asynchronous climate sensitivity between radial growth and isotopes and nonsignificant correlations between RWI and $\delta^{13}C_c$ (Figure 3b) reflect a decoupling between carbon sink and source processes in more arid environments such as in the south.

Understanding growth response to previous climate conditions

The role of carbon reserves for growth initiation The lagged response of growth to previous climate conditions could be related to the use of previously synthesized carbon reserves (e.g., starch) for radial growth (Fritts 1971, Dietze et al. 2014). Therefore, relationships between tree-ring $\delta^{13}C$ and prior-year climate could be expected. However, our results indicated that

tree-ring $\delta^{13}C_c$ values in *P. tarapacana* responded mainly to current growing-season climate. This suggests that although some previous-year sugars might have been used for growth initiation, most of the sugars used for tree-ring cellulose synthesis were fixed at leaf level during the current growing season. Cellulose is typically accumulated at the end of the growing season as the principal component of cell walls (Rathgeber et al. 2016). Indeed, the strongest climate signal in $\delta^{13}C_c$ chronologies occurred later in the growing season (JFM). It has been shown that different portions of the ring may be formed from distinctly different carbon and water sources (Belmecheri et al. 2018, Szejner et al. 2018). Thus, a potential bias toward mid- to latewood in our results may be masking the prior- to early-growing season signal. In *Polylepis*, unfortunately, the extremely small size of the rings (Table 2) may prevent intra-ring analysis of $\delta^{13}C$.

Previous-year conditions may also indirectly determine stem growth over the current growing season, although this may not be imprinted in cellulose material. In evergreen species, older foliage or twigs can have an important role in providing carbon reserves and freshly produced photoassimilates to new shoots and leaves at the beginning of the growing season (Hansen and Beck 1994, Palacio et al. 2018). The preformation of tissues, such as buds (Magnin et al. 2014), foliage or root system in a favorable prior-year could lead to greater carbon assimilation during the current growing season (Loescher et al. 1990, Bréda and Granier 1996). In other words, the importance of prior-year PP on current-year growth could be related to the use of carbon reserves that may improve the canopy and root apparatus for an early and vigorous onset of the growing season. Despite this, our results highlight the importance of current growing-season carbohydrates for mid- to late-season xylem formation.

Tracking *P. tarapacana* photoassimilate pathways using labeled $\delta^{13}C$ and $\delta^{18}O$ (e.g., Kagawa et al. 2006) or radiocarbon (^{14}C) 'bomb spike' dating (Carbone et al. 2013) should be considered for future studies to understand the temporal allocation of carbon to distinct tree components such as buds, foliage, roots or trunk.

Soil moisture as a possible buffer for growth initiation Moisture is essential for the initiation of growth in spring. Water accumulated in the soil after a favorable previous growing season may act as a buffer, allowing trees to use soil water reserves at the start of the growing season before the rainy season starts.

Similar to the climate response of tree-ring $\delta^{13}C_c$, in all the study sites, the correlation between tree-ring $\delta^{18}O$ and climate was strongest with current growing-season climate conditions indicating that trees mostly used water from current growing-season rainfall for cellulose synthesis. Albeit weaker than in the current season, $\delta^{18}O$ also showed a previous growing-season climate signal. This may indicate some use of prior-year water for cellulose synthesis. Given that previous growing-season climate determines in large proportion how much the trees will grow, accumulated water reserves in the soil from previous season may be important for allowing trees to start growing in spring. These soil water reserves may be key for triggering cell division and elongation when temperature threshold for meristematic activity is achieved, probably around October–November, before the actual arrival of rain during the wet season in December. Therefore, this soil water may allow for the initiation of annual growth that will finally determine the total ring width during the growing season, particularly in arid environments. The more the PP and the lower the T in the previous seasons, the greater the water buffer.

Close to our GUA site, *P. tarapacana* grows on sandy soils where water is retained during winter (personal observations). Our field observations indicate that on the sampling sites the trees have shallow root system and grow on shallow rocky soils with low water-holding capacity, but no measurements have been performed on these variables. If some water is retained from one year to the next at our study sites, it can be hypothesized that xylem activity may rely on the climate conditions during the previous year that regulate the availability of water at the start of the growing season. The observed higher dependence on previous-year water availability at the southern-drier sites compared with the northern-wetter sites can be expected since soil water reserves are probably much lower in the south due to lower cloud cover, less PP and higher evaporation. More information is needed regarding *P. tarapacana* root system and soil depth to test this hypothesis. Planned experimental designs including observations of root depth, seasonal changes in cambial activity and soil water content will significantly enhance our understanding of the temporal relations between climate and xylogenesis.

Conclusions

- Both temperature and precipitation exerted a significant influence on tree growth for *Polylepis tarapacana,* the species that constitutes the world's highest treeline. Interannual radial growth of *P. tarapacana* was primarily influenced by water availability during the prior growing season at the drier sites, while T in the current growing season limited radial growth at the northern-wetter sites. This indicates that current growing-season T controls growth at high elevations to the extent as water needs are met.
- We observed a shared response to current climatic conditions for both $\delta^{13}C_c$ and $\delta^{18}O$ tree-ring data, which indicates that tree-ring cellulose is built mainly using carbohydrates assimilated during the current growing season at the four study sites.
- Significant correlations between $\delta^{13}C_c$ and $\delta^{18}O$ chronologies at all study sites may indicate an overall regulation via stomatal conductance of carbon assimilation for *P. tarapacana.* The strength of this stomatal dominance is greater at the southern-drier sites when aridity increases.

- The coupling between carbon source and sink processes (i.e., strong correlations between RWI and $\delta^{13}C_c$) in the northern sites may be related to synchronous current-climate conditions influencing wood formation and leaf gas exchange. By contrast, the decoupling in the southern sites (i.e., non-significant correlations between RWI and $\delta^{13}C_c$) could be the result of prior- and current-climate driving wood formation and leaf gas exchange, respectively.
- While tree growth at drier sites may be more limited under a potentially drier and warmer Altiplano, northern-wetter sites may be more resilient, increasing their stomatal regulation and becoming more PP limited, more similar to the present-day southern sites.
- Carbon reserves and soil water remaining in the soil could be critical factors for growth initiation after cambium dormancy and thus explain two possible mechanisms for understanding growth response to climate conditions in the previous year.

Supplementary data

Supplementary data for this article are available at *Tree Physiology* Online.

Acknowledgments

This paper is dedicated to the memory of Jaime Argollo, who pioneered dendrochronological studies in *Polylepis* in the Andean Cordillera and installed the first Dendrochronology Laboratory in Bolivia in the Universidad Mayor de San Andrés, La Paz. We thank Jaime Argollo, Claudia Soliz and and Jeanette Pacajes for ring-width chronologies development, Wei Wang and Rose Oelkers for lab assistance, Caroline Leland and Benjamin Gaglioti for help with R code, Edward Cook, and the members of the Tree-Ring Lab at Lamont-Doherty Earth Observatory for useful discussions of results. We thank Mathias Vuille and Katia Fernandes for helping with climate data, and Mathias Vuille Françoise Vimeux for discussion regarding $\delta^{18}O$ in Andean precipitation. We acknowledge the Chilean Forest Service CONAF for permission to collect the tree-ring samples in Las Vicuñas National Reserve. The constructive comments of three anonymous reviewers significantly improved the interpretation of our results and the quality of this manuscript. This is Lamont-Doherty Earth Observatory contribution number #8472.

Funding

This research was supported by the project THEMES funded by Fondation BNP Paribas Climate Initiative program; United States National Science Foundation (OISE-1743738, PLR-1504134, AGS-1702789 and AGS 1903687); Lamont-Doherty Earth Observatory Climate Center; Columbia University's Center for Climate and Life; Fondo Nacional de Desarrollo Científico y Tecnológico (FONDECYT 1201411 and 1171640); Agencia Nacional de Investigación y Desarrollo, Fondo de Financiamiento de Centros de Investigación en Áreas Prioritarias (FONDAP 15110009); Agencia Nacional de Promoción Científica y Tecnológica (PICT 2013-1880 and PICT 2018-03691); Consejo Nacional de Investigaciones Científicas y Técnicas de Argentina (PIP CONICET 11220130100584); Proyecto Fondo Nacional de Desarrollo Científico, Tecnológico y de Innovación Tecnológica a Banco Mundial (FONDECYT-BMINC. INV 039-2019).

Authors' contributions

M.R.-C., L.A.-H., M.S.M., V.D., D.A.C. and R.V. conceived and designed the experiment; M.R.-C. performed statistical analyses and wrote the manuscript; L.A.-H. contributed substantially to manuscript elaboration data interpretation, and revisions; V.D., D.A.C., M.S.M., R.V., R.E.C. and M.P.R. contributed substantially to revisions. M.R.-C., M.S.M., D.A.C., C.A., D.A. and F.F. collected and processed data.

Conflict of interest

None declared.

References

Andreu L, Planells O, Gutiérrez E, Helle G, Schleser GH (2008) Climatic significance of tree-ring width and δ13C in a Spanish pine forest network. Tellus B Chem Phys Meteorol 60:771–781.

Andreu-Hayles L, Levesque M, Martin-Benito D et al. (2019) A high yield cellulose extraction system for small whole wood samples and dual measurement of carbon and oxygen stable isotopes. Chem Geol 504:53–65.

Argollo J, Solíz C, Villalba R (2004) Dendrocronological potential of *Polylepis tarapacana* in the Central Andes of Bolivia. Ecología en Bolivia 39:5–24.

Awada T, Skolaut K, Battipaglia G et al. (2019) Tree-ring stable isotopes show different ecophysiological strategies in native and invasive woody species of a semiarid riparian ecosystem in the Great Plains of the United States. Ecohydrology 12:1–13.

Azocar A, Rada F, Garcia-Nuñez C (2007) Functional characteristics of the arborescent genus. Interciencia 32:663–668.

Barbour MM (2007) Stable oxygen isotope composition of plant tissue: a review. Funct Plant Biol 34:83–94.

Begum S, Kudo K, Rahman MH et al. (2018) Climate change and the regulation of wood formation in trees by temperature. Trees Struct Funct 32:3–15.

Belmecheri S, Wright WE, Szejner P, Morino KA, Monson RK (2018) Carbon and oxygen isotope fractionations in tree rings reveal interactions between cambial phenology and seasonal climate. Plant Cell Environ 41:2758–2772.

Biondi F, Waikul K (2004) DENDROCLIM2002: a C++ program for statistical calibration of climate signals in tree-ring chronologies. Comput Geosci 30:303–311.

Braun G (1997) The use of digital methods in assessing forest patterns in an Andean environment: the *Polylepis* example. Mt Res Dev 17:253–262.

Bréda N, Granier A (1996) Intra- and interannual variations of transpiration, leaf area index and radial growth of a sessile oak stand (*Quercus petraea*). Ann For Sci 4:521–536.

Bunn AG (2008) A dendrochronology program library in R (dplR). Dendrochronologia 26:115–124.
Carbone MS, Czimczik CI, Keenan TF, Murakami PF, Pederson N, Schaberg PG, Xiaomei X, Richardson AD (2013) Age, allocation and availability of nonstructural carbon in mature red maple trees. New Phytol 200:1145–1155.
Cernusak LA, Ubierna N, Winter K, Holtum JAM, Marshall JD, Farquhar GD (2013) Environmental and physiological determinants of carbon isotope discrimination in terrestrial plants. New Phytol 200: 950–965.
Christie DA, Lara A, Barichivich J, Villalba R, Morales MS, Cuq E (2009) El Niño-southern oscillation signal in the world's highest-elevation tree-ring chronologies from the Altiplano, Central Andes. Palaeogeogr Palaeoclimatol Palaeoecol 281:309–319.
Cook ER (1985) A time series analysis approach to tree ring standardization. Dissertation. University of Arizona.
Cook ER, Briffa K, Shiyatov S, Mazepa V (1990) Tree-ring standardization and growth-trend estimation. In: Cook ER, Kairiukstis LA (eds) Methods of Dendrochronology: Applications in the Environmental Sciences. Springer Science and Business Media, Dordrecht, pp. 104–123.
Cuyckens GAE, Renison D (2018) Ecología y conservación de los bosques montanos de *Polylepis*: Una introducción al número especial. Ecol Austral 28:157–162.
Cuyckens GAE, Christie DA, Domic AI, Malizia LR, Renison D (2016) Climate change and the distribution and conservation of the world's highest elevation woodlands in the south American Altiplano. Glob Planet Chang 137:79–87.
D'Arrigo R, Wilson R, Liepert B, Cherubini P (2008) On the 'divergence problem' in northern forests: a review of the tree-ring evidence and possible causes. Glob Planet Chang 60:289–305.
Dansgaard W (1964) Stable isotopes in precipitation. Tellus 16:436–468.
Dee DP, Uppala SM, Simmons AJ et al. (2011) The ERA-interim reanalysis: configuration and performance of the data assimilation system. Q J R Meteorol Soc 137:553–597.
Dietze MC, Sala A, Carbone MS, Czimczik CI, Mantooth JA, Richardson AD, Vargas R (2014) Nonstructural carbon in woody plants. Annu Rev Plant Biol 65:667–687.
Domic AI, Capriles JM (2009) Allometry and effects of extreme elevation on growth velocity of the Andean tree *Polylepis tarapacana* Philippi (Rosaceae). Plant Ecol 205:223–234.
Farquhar GD, O'Leary MH, Berry JA (1982) On the relationship between carbon isotope discrimination and the intercellular carbon dioxide concentration in leaves. Aust J Plant Physiol 9:121–137.
Francey RJ, Farquhar GD (1982) An explanation of C13/C12 variations in tree rings. Nature 297:28–31.
Frank DC, Poulter B, Saurer M, Esper J, Huntingford C, Helle G, Treydte K (2015) Water-use eficiency and transpiration across European forests during the anthropocene. Nat Clim Chang 5:579–583.
Fritts HC (1971) Dendroclimatology and dendroecology. Quat Res 1:419–449.
Funk C, Peterson P, Landsfeld M et al. (2015) The climate hazards infrared precipitation with stations - a new environmental record for monitoring extremes. Scientific Data 2:1–21.
Garcia M, Raes D, Jacobsen SE, Michel T (2007) Agroclimatic constraints for rainfed agriculture in the Bolivian Altiplano. J Arid Environ 71:109–121.
Garcia-Nuñez C, Rada F, Boero C, Gonzalez J, Gallardo M, Azocar A, Liberman-Cruz M, Hilal M, Prado F (2004) Leaf gas exchange and water relations in *Polylepis tarapacana* at extreme altitudes in the Bolivian Andes. Photosynthetica 42:133–138.
García-Plazaola JI, Rojas R, Christie DA, Coopman RE (2015) Photosynthetic responses of trees in high-elevation forests: comparing evergreen species along an elevation gradient in the Central Andes. AoB Plants 7:1–13.
Garreaud R, Vuille M, Clement AC (2003) The climate of the Altiplano: observed current conditions and mechanisms of past changes. Palaeogeogr Palaeoclimatol Palaeoecol 194:5–22.
Gehre M, Strauch G (2003) High-temperature elemental analysis and pyrolysis techniques for stable isotope analysis. Rapid Commun Mass Spectrom 17:1497–1503.
Gessler A, Ferrio JP, Hommel R, Treydte K, Werner RA, Monson RK (2014) Stable isotopes in tree rings: towards a mechanistic understanding of isotope fractionation and mixing processes from the leaves to the wood. Tree Physiol 34:796–818.
Gonzalez JA, Liberman-Cruz M, Boero C, Gallardo M, Prado FE (2002) Leaf thickness, protective and photosynthetic pigments and carbohydrate content in leaves of the world's highest elevation tree *Polylepis tarapacana* (Rosaceae). Phyton Int J Exp Botany 71:41–53.
Gosling WD, Hanselman JA, Knox C et al. (2009) Long-term drivers of change in *Polylepis* woodland distribution in the Central Andes. J Veg Sci 20:1041–1052.
Grams TEE, Kozovits AR, Häberle KH, Matyssek R, Dawson TE (2007) Combining δ13C and δ18O analyses to unravel competition, CO2 and O3 effects on the physiological performance of different-aged trees. Plant Cell Environ 30:1023–1034.
Grießinger J, Bräuning A, Helle G, Schleser GH, Hochreuther P, Meier WJH, Zhu H (2019) A dual stable isotope approach unravels common climate signals and species-specific responses to environmental change stored in multi-century tree-ring series from the Tibetan plateau. Geosciences 9:4–6.
Hansen J, Beck E (1994) Seasonal changes in the utilization and turnover of assimilation products in 8-year-old Scots pine (*Pinus sylvestris* L.) trees. Trees 8:172–182.
Hassiotou F, Evans JR, Ludwig M, Veneklaas EJ (2009) Stomatal crypts may facilitate diffusion of CO2 to adaxial mesophyll cells in thick sclerophylls. Plant Cell Environ 32:1596–1611.
Haworth M, McElwain J (2008) Hot, dry, wet, cold or toxic? Revisiting the ecological significance of leaf and cuticular micromorphology. Palaeogeogr Palaeoclimatol Palaeoecol 262:79–90.
Hoch G, Körner C (2005) Growth, demography and carbon relations of *Polylepis* trees at the world's highest treeline. Funct Ecol 19:941–951.
Jordan GJ, Weston PH, Carpenter RJ, Dillon RA, Brodribb TJ (2008) The evolutionary relations of sunken, covered, and encrypted stomata to dry habitats in Proteaceae. Am J Bot 95:521–530.
Kagawa A, Sugimoto A, Maximov TC (2006) 13CO2 pulse-labelling of photoassimilates reveals carbon allocation within and between tree rings. Plant Cell Environ 29:1571–1584.
Kessler M (1995) Present and potential distribution of *Polylepis* (Rosaceae) forests in Bolivia. In: Churchill SP, Balslev H, Forero E, Luteyn JL (eds) Biodiversity and conservation of neotropical montane forests. New York Botanical Garden, New York, NY, pp. 281–294.
Kessler M, Böhner J, Kluge J (2007) Modelling tree height to assess climatic conditions at tree lines in the Bolivian Andes. Ecol Model 207:223–233.
Kleier C, Rundel PW (2004) Microsite requirements, population structure and growth of the cushion plant *Azorella compacta* in the tropical Chilean Andes. Austral Ecol 29:461–470.
Körner C (1998) A re-assessment of high elevation treeline positions and their explanation. Oecologia 115:445–459.
Körner C (2003) Carbon limitation in trees. J Ecol 91:4–17.
Körner C (2015) Paradigm shift in plant growth control. Plant Biol 25:107–114.
Körner C, Farquhar GD, Roksandic Z (1988) A global survey of carbon isotope discrimination in plants from high altitude. Oecologia 74:623–632.

Lavergne A, Daux V, Pierre M, Stievenard M, Srur AM, Villalba R (2018) Past summer temperatures inferred from dendrochronological records of *Fitzroya cupressoides* on the eastern slope of the northern Patagonian Andes. J Geophys Res Biogeo sci 123:32–45.

Lavergne A, Voelker S, Csank A et al. (2020) Historical changes in the stomatal limitation of photosynthesis: empirical support for an optimality principle. New Phytol 225:2484–2497.

Leuenberger M (2007) To what extent can ice core data contribute to the understanding of plant ecological developments of the past? New Phytol 1:211–233.

Liang E, Dawadi B, Pederson N, Eckstein D (2014) Is the growth of birch at the upper timberline in the Himalayas limited by moisture or by temperature? Ecology 95:2453–2465.

Loescher WH, Mccamant T, Keller JD (1990) Carbohydrate reserves, translocation, and storage in woody plant roots. HortScience 25:274–281.

López VL, Cellini JM, Cuyckens GAE. (2021). Influencia del micrositio y el ambiente en la instalación de *Polylepis tarapacana* en los Altos Andes. Neotrop Biodivers 7:135–145.

Macek P, Macková J, de Bello F (2009) Morphological and ecophysiological traits shaping altitudinal distribution of three *Polylepis* treeline species in the dry tropical Andes. Acta Oecol 35:778–785.

Magnin A, Puntieri J, Villalba R (2014) Interannual variations in primary and secondary growth of *Nothofagus pumilio* and their relationships with climate. Trees 28:1463–1471.

Meko DM, Touchan R, Anchukaitis KJ (2011) Seascorr: a MATLAB program for identifying the seasonal climate signal in an annual tree-ring time series. Comput Geosci 37:1234–1241.

Minvielle M, Garreaud RD (2011) Projecting rainfall changes over the south American Altiplano. J Clim 24:4577–4583.

Morales MS, Villalba R, Grau HR, Paolini L (2004) Rainfall-controlled tree growth in high-elevation subtropical treelines. Ecology 85:3080–3089.

Morales MS, Christie DA, Villalba R, Argollo J, Pacajes J, Silva JS, Alvarez CA, Llancabure JC, Solíz Gamboa CC (2012) Precipitation changes in the south American Altiplano since 1300 AD reconstructed by tree-rings. Clim Past 8:653–666.

Morales MS, Carilla J, Grau HR, Villalba R (2015) Multi-century lake area changes in the southern Altiplano: a tree-ring-based reconstruction. Clim Past 11:1139–1152.

Morales MS, Cook ER, Barichivich J et al. (2020) 600 years of south American tree rings reveal an increase in severe hydroclimatic events since mid-20th century. Proc Natl Acad Sci USA 117:1–48.

Moya J, Lara A (2011) Tree rings chronologies of quenoa (*Polylepis tarapacana*) for the last 500 years in the Altiplano of Arica and Parinacota region. Chile Bosque 32:165–173.

Muller B, Pantin F, Génard M, Turc O, Freixes S, Piques M, Gibon Y (2011) Water deficits uncouple growth from photosynthesis, increase C content, and modify the relationships between C and growth in sink organs. J Exp Bot 62:1715–1729.

Neukom R, Rohrer M, Calanca P, Salzmann N, Huggel C (2015) Facing unprecedented drying of the Central Andes? Precipitation variability over the period AD 1000 – 2100. Environ Res Lett 10:084017.

O'Leary MH (1988) Carbon isotopes in photosynthesis. Bioscience 38:328–336.

Palacio S, Hoch G, Sala A, Körner C, Millard P (2014) Does carbon storage limit tree growth? New Phytol 201:1096–1100.

Palacio S, Camarero JJ, Maestro M, Alla AQ, Lahoz E, Montserrat-Martí G (2018) Are storage and tree growth related? Seasonal nutrient and carbohydrate dynamics in evergreen and deciduous Mediterranean oaks. Trees Struct and Funct 32:777–790.

Piper FI, Fajardo A (2011) No evidence of carbon limitation with tree age and height in *Nothofagus pumilio* under mediterranean and temperate climate conditions. Ann Bot 108:907–917.

Prentice I, Dong N, Gleason SM, Maire V, Wright IJ (2014) Balancing the costs of carbon gain and water transport: testing a new theoretical framework for plant functional ecology. Ecol Lett 17:82–91.

R Development Core Team. (2020). R: A language and environment for statistical computing. R Foundation for Statistical Computing, Vienna, Austria. https://www.R-project.org/.

Rada F, Garcia-Nuñez C, Boero C, Gallardo M, Hilal M, González J, Prado F, Liberman-Cruz M, Azócar A (2001) Low-temperature resistance in *Polylepis tarapacana*, a tree growing at the highest altitudes in the world. Plant Cell Environ 24:377–381.

Rahman MH, Nugroho WD, Nakaba S, Kitin P, Kudo K, Yamagishi Y, Begum S, Marsoem SN, Funada R (2019) Changes in cambial activity are related to precipitation patterns in four tropical hardwood species grown in Indonesia. Am J Bot 106:760–771.

Rathgeber CBK, Cuny HE, Fonti P (2016) Biological basis of tree-ring formation: a crash course. Front Plant Sci 7:1–7.

Ren P, Rossi S, Camarero JJ, Aaron M, Ellison AM, Eryuan Liang E, Peñuelas J (2018) Critical temperature and precipitation thresholds for the onset of xylogenesis of *Juniperus przewalskii* in a semi-arid area of the north-eastern Tibetan plateau. Ann Bot 121:617–624.

Requena-Rojas EJ, Morales M, Villalba R (2020) Dendroclimatological assessment of *Polylepis rodolfo-vasquezii*: a novel *Polylepis* species in the Peru highlands. Dendrochronologia 62:125722.

Requena-Rojas EJ, Taquire Arroyo A (2019) Anatomía del leño y caracterización de los anillos de crecimiento en individuos de *Polylepis tarapacana* en el Altiplano-Tacna-Perú. Quebracho 27:66–75.

Roden JS, Lin G, Ehleringer JR (2000) A mechanistic model for interpretation of hydrogen and oxygen isotope ratios in tree-ring cellulose. Geochim Cosmochim Acta 64:21–35.

Rossi S, Deslauriers A, Griçar J et al. (2008) Critical temperatures for xylogenesis in conifers of cold climates. Glob Ecol Biogeogr 17:696–707.

Samuels-Crow K, Galewsky J, Hardy DR, Sharp ZD, Worden J, Braun C (2014) Upwind convective influences on the isotopic composition of atmospheric water vapor over the tropical Andes. J Geophys Res Atmos 119:7051–7063.

Saurer M, Siegwolf RTW, Schweingruber FH (2004) Carbon isotope discrimination indicates improving water-use efficiency of trees in northern Eurasia over the last 100 years. Glob Chang Biol 10:2109–2120.

Scheidegger Y, Saurer M, Bahn M, Siegwolf R (2000) Linking stable oxygen and carbon isotopes with stomatal conductance and photosynthetic capacity: a conceptual model. Oecologia 125: 350–357.

Shi P, Körner C, Hoch G (2008) A test of the growth limitation theory for alpine tree line formation in evergreen and deciduous taxa of the eastern Himalayas. Funct Ecol 22:213–220.

Simpson BB (1979) A revision of the genus *Polylepis* (Rosaceae: Sanguisorbeae). Smithson Contrib Bot 43:1–62.

Soliz C, Villalba R, Argollo J, Morales MS, Christie DA, Moya J, Pacajes J (2009) Spatio-temporal variations in *Polylepis tarapacana* radial growth across the Bolivian Altiplano during the 20th century. Palaeogeogr Palaeoclimatol Palaeoecol 281:296–308.

Suess H (1955) Radiocarbon concentration in modern wood. Science 122:415–417.

Szejner P, Wright WE, Belmecheri S, Meko D, Leavitt SW, Ehleringer JR, Monson RK (2018) Disentangling seasonal and interannual legacies from inferred patterns of forest water and carbon cycling using tree-ring stable isotopes. Glob Chang Biol 24:5332–5347.

Thibeault J, Seth A, Wang G (2012) Mechanisms of summertime precipitation variability in the Bolivian Altiplano: present and future. Int J Climatol 32:2033–2041.

Toivonen JM, Horna V, Kessler M, Ruokolainen K, Hertel D (2014) Interspecific variation in functional traits in relation to species climatic

niche optima in Andean *Polylepis* (Rosaceae) tree species: evidence for climatic adaptations. Funct Plant Biol 41:301–312.

van der Schrier G, Barichivich J, Briffa KR, Jones PD (2013) A scPDSI based global data set of dry and wet spells for 1901–2009. J Geophys Res Atmos 118:4025–4048.

Vuille M, Bradley RS (2000) Mean annual temperature trends and their vertical structure in the tropical Andes. Geophys Res Lett 27:3885–3888.

Vuille M, Keimig F (2004) Interannual variability of summertime convective cloudiness and precipitation in the Central Andes derived from ISCCP-B3 data. J Clim 17:3334–3348.

Vuille M, Bradley RS, Keimig F (2000) Interannual climate variability in the Central Andes and its relation to tropical Pacific and Atlantic forcing. J Geophys Res 105:447–460.

Vuille M, Bradley RS, Werner M, Healy R, Keimig F (2003) Modeling δ18O in precipitation over the tropical Americas: 1. Interannual variability and climatic controls. J Geophys Res Atmos 108:4174.

Vuille M, Franquist E, Garreaud R, Lavado Casimiro WS, Cáceres B (2015) Impact of the global warming hiatus on Andean temperature. J Geophys Res Atmos 120:3745–3757.

Wigley TML, Briffa KR, Jones PD (1984) On the average value of correlated time series, with applications in dendroclimatology and hydrometeorology. J Clim Appl Meteorol 23: 201–213.

Wright IJ, Reich PB, Westoby M (2003) Least-cost input mixtures of water and nitrogen for photosynthesis. Am Nat 161:98–111.

Zang C, Biondi F (2015) Treeclim: an R package for the numerical calibration of proxy-climate relationships. Ecography 38:431–436.

Zutta BR, Rundel PW (2017) Modeled shifts in *Polylepis* species ranges in the Andes from the last glacial maximum to the present. Forests 8:1–16.